DESIGN OF A SWEEPING IMPEDANCE PROBE FOR THE SPORT MISSION

by

Caleb W. Young

A thesis submitted in partial fulfillment
of the requirements for the degree

of

MASTER OF SCIENCE

in

Electrical Engineering

Approved:

Charles M. Swenson, Ph.D. Major Professor	Jonathan D. Phillips, Ph.D. Committee Member
Jacob Gunther, Ph.D. Committee Member	Janis L. Boettinger, Ph.D. Acting Vice Provost of Graduate Studies

UTAH STATE UNIVERSITY
Logan, Utah

2020

ABSTRACT

Design of a Sweeping Impedance Probe for the SPORT Mission

by

Caleb W. Young, Master of Science

Utah State University, 2020

Major Professor: Charles M. Swenson, Ph.D.
Department: Electrical and Computer Engineering

In our modern world satellite systems are an evermore common part of day to day life. Reliable communication from the ground to these satellites is becoming more and more necessary. Plasma scintillations in the ionosphere can make these communications difficult or even impossible. By gaining a better understanding of these scintillations, times of bad satellite connection can be predicted in the same way terrestrial weather gets predicted and reported today. The objective of the SPORT mission is to gain a better understanding of these plasma scintillations. In order to measure plasma density, and gain a better understanding of plasma scintillations, a Sweeping Impedance Probe (SIP) can be used.

It is proposed that the SIP for the SPORT mission be a digital rework of a probe used on the ASSP mission. By using digital processing methods instead of analog methods the new probe can be more accurate in the plasma measurement.

This thesis will describe the theory and design of the SPORT SIP and its advantages over previous analog methods. The design is detailed for both the analog and digital portions of the probe along with a selection of testing data. Potential changes are also discussed.

(67 pages)

PUBLIC ABSTRACT

Design of a Sweeping Impedance Probe for the SPORT Mission

Caleb W. Young

In our modern world satellite systems are an evermore common part of day to day life. Reliable communication from the ground to these satellites is becoming more and more necessary. Plasma scintillations in the ionosphere can make these communications difficult or even impossible. By gaining a better understanding of these scintillations, times of bad satellite connection can be predicted in the same way terrestrial weather gets predicted and reported today. The objective of the SPORT mission is to gain a better understanding of these plasma scintillations. In order to measure plasma density, and gain a better understanding of plasma scintillations, a Sweeping Impedance Probe (SIP) can be used.

It is proposed that the SIP for the SPORT mission be a digital rework of a probe used on the ASSP mission. By using digital processing methods instead of analog methods the new probe can be more accurate in the plasma measurement.

This thesis will describe the theory and design of the SPORT SIP and its advantages over previous analog methods. The design is detailed for both the analog and digital portions of the probe along with a selection of testing data. Potential changes are also discussed.

ACKNOWLEDGMENTS

First off I need to thank Dr. Swenson. His guidance as I have worked through my entire masters program and this project has been invaluable. Just being able to work on the SPORT project was probably the most important part of all of my time at school. My abilities as an engineer would not be anywhere near what they are now without this chance to gain experience on a real project. So much that I and the other students learned came from the time that Dr. Swenson was able to give us in his endlessly busy schedule.

I also need to thank all the other students that were involved on this project. Nathan Tipton and Jordan Haws and I starting down this road the same day. We worked on all of the instruments, not just the impedance probe. Without them there is no impedance probe, no USU space weather instrument for that matter. So much of both the digital and analog design was from working with Nathan. Many a bug would have been much harder to smash if it weren't for his help. Make sure to check out his thesis on the Langmuir Probe when it gets published. I wish I had a reason to cite it in here.

Then there is Russell Babb, Joel Mork, Dr. Phillips, Lucas Anderson, our friends in Brazil, and Colton Anderson who made my time at the CSE as enjoyable as it was. They all had a hand in what is now a functional set of probes.

And, of course, my wife Emily. Without her this thesis probably wouldn't have gotten finished.

Caleb Young

CONTENTS

LIST OF TABLES

LIST OF FIGURES

ACRONYMS

AC	Alternating Current
ADC	Analog-to-Digital Converter
ASSP	Auroral Spatial Structures Probe
CDS	Correlated Double Sampling
CORDIC	Coordinate Rotation Digital Computer
DAC	Digital-to-Analog Converter
DC	Direct Current
EFP	Electric Field Probe
FFT	Fast Fourier Transform
FIFO	First-In, First-Out
FPGA	Field Programmable Gate Array
GSFC	Goddard Space Flight Center
GPS	Global Positioning System
HSADC	High Speed Analog to Digital Converter
HSDAC	High Speed Digital to Analog Converter
HDL	Hardware Description Language
ITA	Instituto Tecnológico de Aeronáutica
LPF	Low-Pass Filter
LSB	Least Significant Bit
LUT	Look-Up Table
MSB	Most Significant Bit
MSFC	Marshall Space Flight Center
NASA	National Aeronautics and Space Administration
NCO	Numerically Controlled Oscillator
RF	Radio Frequency
R-L-C	Resistive Inductive Capacitive
RTL	Register-transfer Level

PID	Proportional-Integral-Differential
SIP	Sweeping Impedance Probe
SLP	Sweeping Langmuir Probe
SPORT	Scintillation Prediction Observation Research Task
USU	Utah State University
UTD	University of Dallas Texas
VHDL	Very High Speed Integrated Circuit Hardware Description Language
VNA	Vector Network Analyzer

CHAPTER 1

INTRODUCTION

Our lives today are increasingly dependent on satellite systems. These systems provide us services such as global imaging, global positioning, and television broadcasting. All are incredibly useful services in our modern times. The main technology that makes these services possible is the ability to consistently communicate from the earths surface to the satellite. If that communication were to be removed, or just disrupted, these services would be rendered unusable.

One such disruption that causes scintillation on radio transmissions are plasma bubbles that often occur at night in the equatorial region of the Earth's ionosphere. The ionosphere is a layer of the atmosphere that contains high levels of ionized particles, electrons and ions, referred to as plasma. Under normal conditions, the ionosphere has little effect on the passage of radio waves between the earth and the satellites above, because the ionospheric plasma has a very uniform density. The bubbles are pockets of low-density plasma that rise up from the bottom of the ionosphere into the higher density plasma above. When these bubbles appear they produce turbulence in the ionospheric plasma density and the radio waves passing through this turbulence become diffused and can be unusable. This effect can be compared to light passing through water. When the water is still and calm the light passes through with little change, but when there are bubbles present the light becomes scattered and one cannot see through the water anymore. While the plasma bubbles and the turbulence caused by their upward rise persist, satellite communications are often stopped until the ionosphere returns to a calm state.

Over areas of South America plasma bubbles are very common nightly occurrences, posing troubles to industries that depend on satellite communications. For example, precision agriculture, which relies on GPS navigation, has to be stopped when a bubble forms in the ionosphere above. For reasons such as this, being able to understand what triggers and

being able to predict these bubbles is of major interest to countries where plasma bubbles are common.

The scientific community needs observations of the space environment before scientific models can reasonably be developed to predict when bubbles will happen. Observations are needed under all possible conditions including pre-bubble, post-bubble, and during a bubble to understand what triggers bubble formation. The measurements to be made in space by the Scintillation Prediction Observation Research Task (SPORT) spacecraft, along with ground based radars and ionosondes, will provide the data need to develop and test models to predict when these bubbles occur.

1.1 The SPORT Mission

The SPORT mission is a CubeSat mission that is geared toward learning and understanding more about what gives rise to these plasma bubbles and how scintillations are caused by the ionosphere. The mission is a joint science mission between the United States of America (USA) and Brazil. In the USA, Utah State University (USU), University of Dallas Texas (UTD), Marshall Space Flight Center (MSFC), Goddard Space Flight Center (GSFC), and The Aerospace Corporation are all organizations that will develop and fly instruments and payloads to better understand the conditions that give rise to plasma scintillations. In Brazil, the Instituto Teconològico de Aeronàutica (ITA) will be providing the spacecraft, flight computer, while the Instituto Nacional de Pesquisas Espaciais (INPE) will provide communication capabilities and telemetry handling from the ground through their EMBRACE program.

The SPORT program was selected by NASA headquarters in December of 2016 to proceed and funding was made available to the US partners in the fall of 2017. Funding for the Brazil portion of the program occurred in early 2018. The required U.S.-Brazil Framework Agreement was ratified in April 2018 and NASAs Office of International and Interagency worked with the U.S. Embassy in Brazil to press for conclusion of the Implementing Arrangement in early 2019. Delivery of the completed US instruments to Brazil is expected in the summer of 2020 with launch of the spacecraft in fall 2021.

1.2 The SPORT Impedance Probe

Utah State University is providing a suite of three instruments for measuring plasma density and temperature of the ionosphere. The USU payload will consist of two Electric Field Probes (EFP), a Sweeping Langmuir Probe (SLP), and a Sweeping Impedance Probe (SIP). This suite of instruments is referred to as the Space Weather Probes. Other smaller measurement devices will also be included on the Space Weather Probes. A top level diagram of the instrumentation for the Space Weather Probes is shown in Figure 1.1. Both the SIP and the SLP will be used measure the ionospheric plasma density but with very different techniques. Both probes measure the properties of a probe immersed in plasma, but the SIP uses the AC impedance of the probe while the SLP uses the DC resistance to determine the plasma density. An advantage of the SIP technique is that it can determine absolute electron density, irrespective of the payload charging and surface contamination by monitoring the changing impedance of the probe. The SLP is a technically simpler probe to implement but can only reliably measure changes in plasma density and cannot be calibrated to provide an absolute measurement without comparison to some other technique such as the SIP. The impedance probe technique has been used for over fifty years to probe the electron density in the Earths ionosphere on sounding rockets and spacecraft [1–3]. By using both the SLP and the SIP techniques together a more accurate plasma density measurement can be achieved. The two probes will be used to check each other for proper measurements and to provide a fallback for conditions under which one probe may not be operating.

The SIP will be used to determine electron density by monitoring the current supplied to a short monopole antenna when driven with a low-voltage RF signal. The probe length (approx. 30 cm) is a fraction of the free space wave-length of the applied RF signals (1 – 30MHz) such that it has a capacitive impedance. To first order the impedance of the probe is dependent on the average dielectric properties encompassed by the near fields that exist between the probe and the spacecraft. Essentially, the probe and spacecraft form a complex geometry capacitor that is filled with the ionospheric plasma. The theoretical

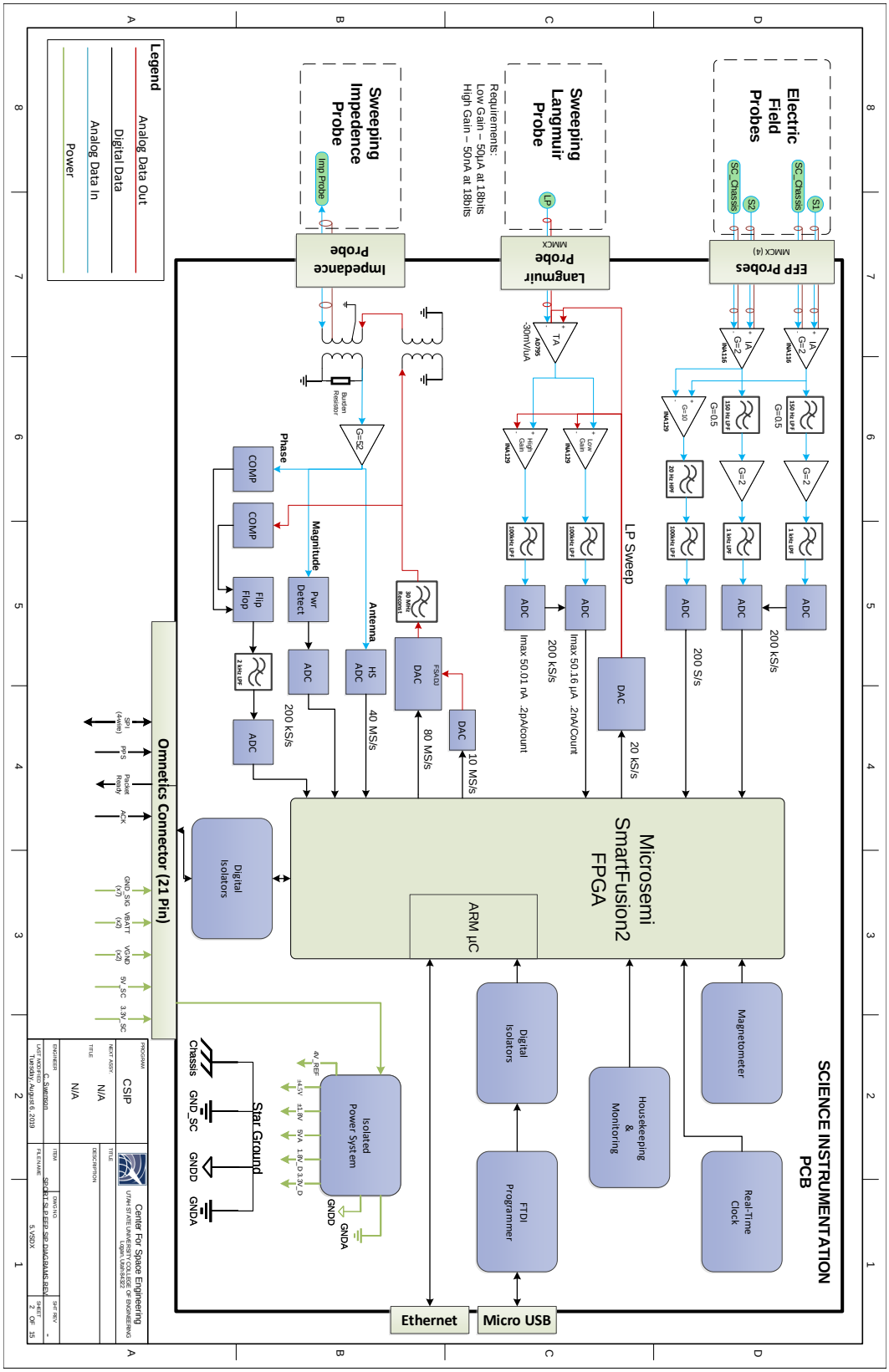

Fig. 1.1: Top Level Diagram of the SPORT Space Weather Instrument

impedance of such probes has been studied extensively [4–7] along with their use as a plasma diagnostic [8–10]. A probe's impedance can change by factors of 20 in magnitude and 180 degrees in phase from its free space values over nominal ionospheric density ranges. The dielectric properties of the plasma modify the capacitive impedance of the probe into a complex response characterized by two resonances. The lower frequency resonance has the characteristics of a series R-L-C circuit resonance while the higher frequency has a parallel R-L-C circuit characteristic. The series resonance occurs at the electron gyro frequency modified by the capacitance of the plasma sheath surrounding the probe spacecraft system. The parallel resonance occurs at the upper hybrid frequency which is determined by the electron density and magnetic field magnitude.

1.3 Literature Review

The Sweeping Impedance Probe for the SPORT mission is primarily based on the design implemented on the ASSP mission. The ASSP mission will be discussed and reviewed here.

1.3.1 The ASSP Mission

The Auroral Spatial Structures Probe (ASSP) was a NASA-sponsored sounding rocket mission that was launched in early 2015. The sounding rocket was launched to study what happens to the Earth's electric and magnetic fields during an aurora [11]. The rocket contained six sub-payloads that were ejected during flight and one main payload attached to the rocket itself. Each payload included a Langmuir Probe, Magnetometer, Electric Field Probe, and a GPS receiver. Additionally, the main payload also contained a modified Langmuir Probe and an Impedance Probe [11, 12]. The design for the ASSP SIP was based on designs for a Vector Network Analyzer (VNA). The operation of a VNA is to output an AC signal to a device and calculate the magnitude and phase of the returning signal compared to the original signal. The reference AC signal generation and the mixing to find the real and imaginary components of returning signal were all done with dedicated analog components. Only the processed signal components were sampled and then sent to the ground [12].

To increase the accuracy of the measurements, the ASSP impedance probe implemented an oversampling method, referred to as Correlated Double Sampling (CDS). The signal from the probe was mixed with two sets of sinusoidal signals, the usual cosine and negative sine signals along with a sine and negative cosine (rotated 180 degrees from the original set). This other set of signals rotates the mixed signal around the complex plane allowing for the analog offset to be calculated and removed by finding the difference between the two mixed signals. If there is no offset, when the secondary mixed signal is subtracted from the first mixed signal the difference will come to zero because they are exactly opposite. If an offset is present the difference between the two signals represents the offset [12].

The possible problem that this method presents is that the probe signals used for the multiple mixing stages were received at different times and locations across the probe's path through space. By using signals from different times and locations a small amount of error is added to the end measurement. This error is small compared to the errors removed by performing CDS.

1.4 Thesis Statement and Research Task

It is proposed to implement the Sweeping Impedance Probe for the SPORT mission as the research component for this Master of Science Degree. The Sweeping Impedance Probe for the SPORT mission will use the in-phase and quadrature (I/Q) detection techniques demonstrated on the ASSP mission. What differentiates the approach for the SIP on the SPORT mission from the impedance probe on the ASSP mission is an increased emphasis on digital signal processing on Field Programmable Gate Arrays (FPGAs) instead of using dedicated analog hardware. The ASSP mission used an analog mixer to shift the measurements at RF frequencies to baseband and to provide I and Q observations. Our proposed approach for the SPORT mission will use a high-speed analog to digital converter to sample the RF-signal and implement the mixing digitally in the FPGA. This digital mixing removes the need for CDS that was used on the ASSP mission. The remaining analog components of the ASSP instrument will be updated to reduce power consumption and decrease noise within the SPORT SIP.

Implementing more of the SIP using digital processing techniques instead of dedicated analog hardware provides the following benefits. First, digital processing approach is less susceptible to degradation and drift over time. Analog components may have characteristics that change from the original calibration due the space environment or aging. Second, digital processing is more flexible and can be changed to be mission specific without having to make all new hardware. All that is needed to change the system is to reprogram the digital components. This proposed shift to digital makes modifying the system for a future mission a simpler task compared to an all analog system.

The thesis statement for the proposed research is: Can a miniature low-power sweeping impedance probe be developed using a high speed analog to digital converter and digital signal processing techniques that meets the SPORT mission science objectives?

1.5 Thesis Outline

The remainder of the thesis will be structured with the following chapters.

Chapter 2 will describe the design requirements that the SIP must meet to be considered successful. This includes high level science requirements and how they were converted to engineering requirements. How the system is designed from these requirements will be discussed.

Chapter 3 will include details of the analog portion of the system. Designs of the analog system will be presented along with reasoning for the design. The analog circuitry for the RF signal handling and conditioning is described with schematic designs.

Chapter 4 discusses details of the design of the digital system. How the FPGA system was designed and all the processing blocks will be shown. The data flow from single data samples to processed data packets will be shown.

Chapter 5 will discuss the testing procedures to verify system functionality.

Chapter 6 will conclude and discuss future work and possible changes to the design.

CHAPTER 2

REQUIREMENTS AND THEORY OF OPERATIONS

2.1 SIP Theory of Operation

The impedance probe technique measures the ionospheric plasma by monitoring the current that flows in response to an RF voltage applied at the input of a probe that is immersed in the plasma. The current response depends on both the probe dimensions and the ionospheric plasma surrounding the probe. The variation of this current response at different frequencies provides a characteristic signature from which ionospheric density can be determined using the theory presented in [4–7].

2.1.1 Signals and Impedances

The ratio of the current response to the stimulating voltage is used for the impedance probe instead of just the current because it removes any variability of the driving voltage signal in the current response. The ratio of the voltage to the current for sinusoidal signals is the impedance of the probe. Electrical impedance is quantified as a complex valued electrical resistance. With real valued resistances, the resistance is defined by Ohms Law as the ratio of the voltage over the current: $R = V/I$. Complex impedances, Z, represent the same ratio, but account for magnitude differences and phase differences between AC voltage and AC current. For example, if an AC voltage signal is $V = 1e^{jwt}$ and the corresponding AC current is $I = 0.5e^{j(wt-90^\circ)}$ then

$$Z = \frac{V}{I} = \frac{e^{jwt}}{0.5e^{j(\omega t-90^\circ)}} = 2e^{j90^\circ}$$

From this result it is easily seen that the magnitude and phase shift from the impedance can be generalized as a complex exponential number

$$Z = Ae^{j\phi}$$

where A is the magnitude gain and ϕ is the phase shift. In the example above this impedance would represent the voltage magnitude being twice the current magnitude, and the voltage phase leads the current phase by 90 degrees. This form is known as the polar form of a complex number. Figure 2.1 gives a visual representation of how impedance affects an AC signal.

This complex exponential representation gives a very convenient way to see what is happening to a signal by showing the magnitude change and the phase change in a single value. By exploiting the simple structure, systems can be designed to calculate the magnitude change and phase change individually to find the impedance.

2.2 Probe Model

The SIP for the SPORT mission will make use of a short monopole probe driven with a low-voltage (10 mV) RF signal. The probe length (30 cm) is a fraction of the free space wavelength of the applied RF signals (1–30MHz) such that it has capacitive impedance. The impedance of the probe immersed in the plasma is dependent on the average dielectric properties encompassed by the near fields that exist between the probe and the spacecraft. Essentially the probe and spacecraft form a complex geometry capacitor that is filled with the ionospheric plasma. The theoretical impedance models have been well defined by previous research [4–7] as well as how they can be used as a plasma diagnostic [8–10]. Magnitude and phase plots of the theoretical impedance seen on the probe with different plasma densities are shown in Figure 2.2.

Using these models as background, measurements from a probe in the plasma can be used to calculate the plasma density at the time of the measurement. It is noted that in the phase plot that as the plasma density increases the frequency at which the impedance

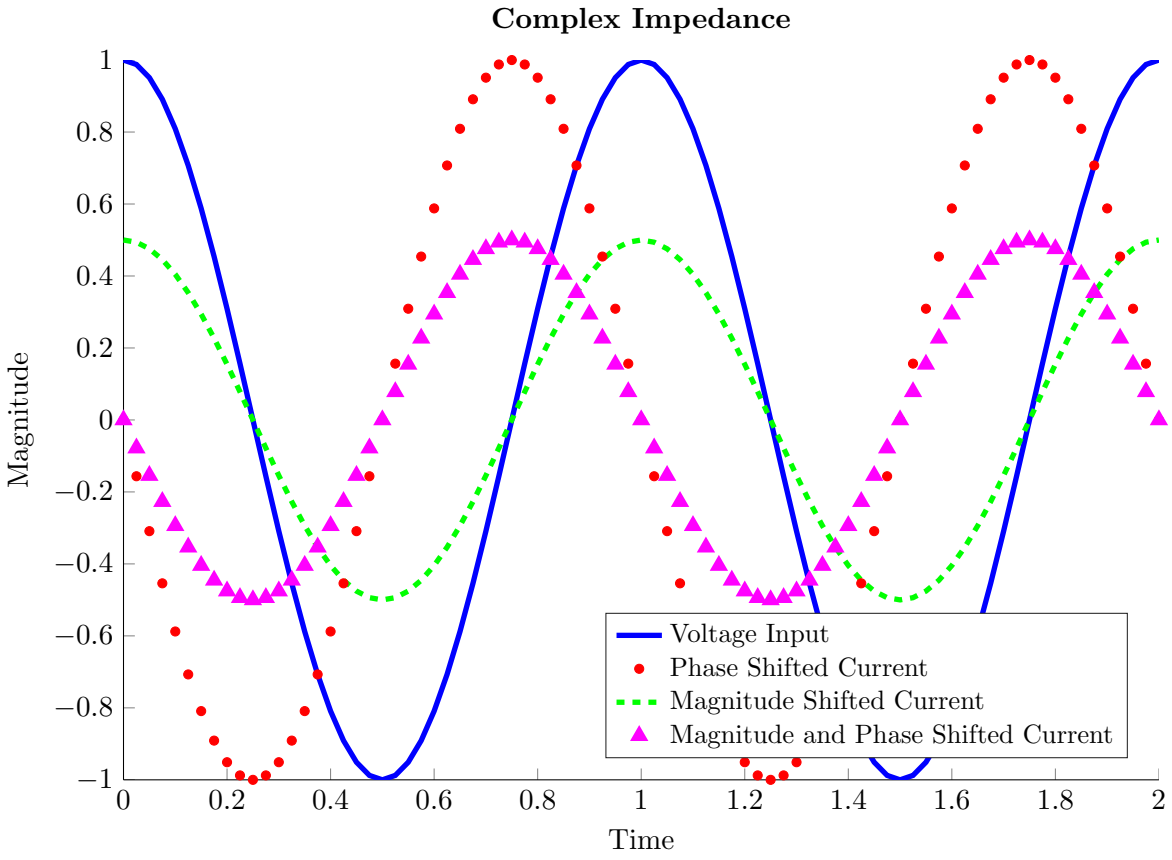

Fig. 2.1: Example of the effects of impedance

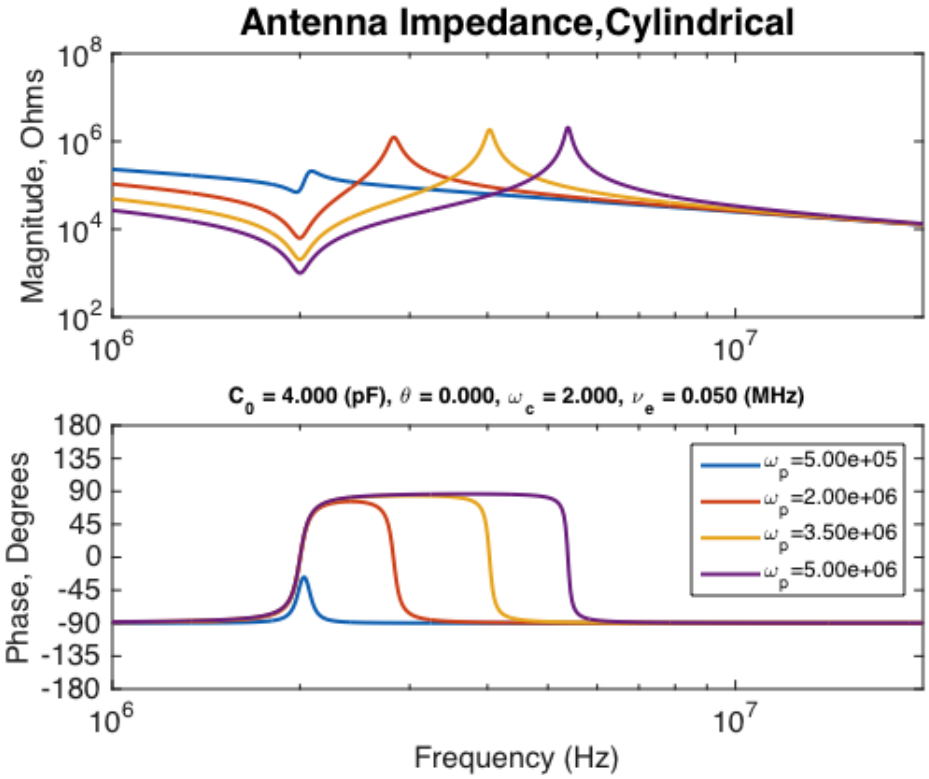

Fig. 2.2: Theoretical impedance characteristics for a cylindrical probe

moves from inductive to capacitive also increases. There is also a maximum value of the magnitude found at the same frequency. This frequency is referred to as the upper hybrid frequency. Finding this upper hybrid frequency will be the primary method of calculating the plasma density.

2.2.1 I/Q Sampling

The complex impedance of the probe in the plasma, Z, can be represented in either polar or rectangular form:

$$Ae^{j\phi} = I + jQ$$

where the relation between I,Q and A, ϕ is given by:

$$A = \sqrt{I^2 + Q^2} \tag{2.1}$$

$$\phi = tan^{-1}\left(\frac{Q}{I}\right) \tag{2.2}$$

$$I = Acos(\phi) \tag{2.3}$$

$$Q = Asin(\phi). \tag{2.4}$$

There are both algorithms and instrumentation to detect either the magnitude/phase or the I/Q representations of the impedance using either analog or digital systems. Both magnitude/phase and I/Q require some type of reference signal to compare against so as to determine the timing of the voltage relative to the current, or phase shift.

The I/Q representation of the impedance is found through the use of multiplication of the signal with a reference signal using either an analog mixer or with digital multiplication, depending where in the signal chain the analog to digital converter is placed. The advent of high sampling speed analog to digital converters (ADCs) allows for the digitization of the RF (1–30MHz) current signal directly. The analog mixer and its non-ideal characteristics are avoided and the I/Q detection can be accomplished using digital processing that is ideal, noise free, and do not drift with temperature. These are the same techniques as commonly

referred to as software-defined radio in which a high speed ADC is followed by digital signal processing algorithms. Because of these advantages the digital I/Q method will be used in the USU SIP to detect the impedance of the probe.

Figure 2.3 shows the implementation of the mixing operation. A derivation of this implementation is as follows.

To calculate the I/Q samples, trigonometric identities are exploited. It is known that

$$cos(\alpha)cos(\beta) = \frac{1}{2}[cos(\alpha+\beta) + cos(\alpha-\beta)]. \tag{2.5}$$

By applying a low-pass filter, the double frequency term can be removed and the remaining signal is

$$cos(\alpha)cos(\beta) \approx \frac{1}{2}[cos(\alpha-\beta)]. \tag{2.6}$$

If the AC current signal returning from the probe, R, is $R = Acos(f+\phi)$ and we have the signals $cos(f)$ and $cos(f+pi/2)$ available then by using Equations 2.3, 2.4, and 2.5 we get:

$$Rcos(f) = \frac{A}{2}cos(\phi) = \frac{I}{2} \tag{2.7}$$

$$Rcos\left(f+\frac{\pi}{2}\right) = \frac{A}{2}[cos\left(\phi-\frac{\pi}{2}\right)] = \frac{A}{2}sin(\phi) = \frac{Q}{2} \tag{2.8}$$

Thus, by taking the received signal and multiplying it with $cos(f)$ and $cos(f+\frac{\pi}{2})$, then filtering, the I/Q data is directly found. This simplicity is what makes using the I/Q method an attractive option for impedance measurements. To implement this approach,

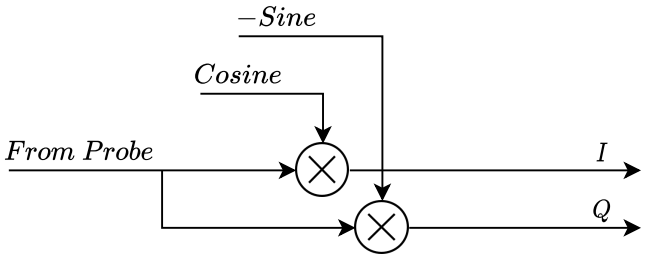

Fig. 2.3: Block diagram of the mixing operation

the $cos(f)$ and $cos(f + \frac{\pi}{2})$ signals will need to be generated along with the output signal. Note that $cos(f + \frac{\pi}{2}) = -sin(f)$.

By using Equations 2.1 and 2.2, the magnitude/phase can be found if needed as

$$\sqrt{\frac{I}{2}^2 + \frac{Q}{2}^2} = A/2 \tag{2.9}$$

$$tan^{-1}\left(\frac{\frac{Q}{2}}{\frac{I}{2}}\right) = \phi. \tag{2.10}$$

Lingering scale factors can be compensated for in calibration if needed.

2.2.2 System Overview

The full SIP system to find the I/Q samples is shown in Figure 2.4.

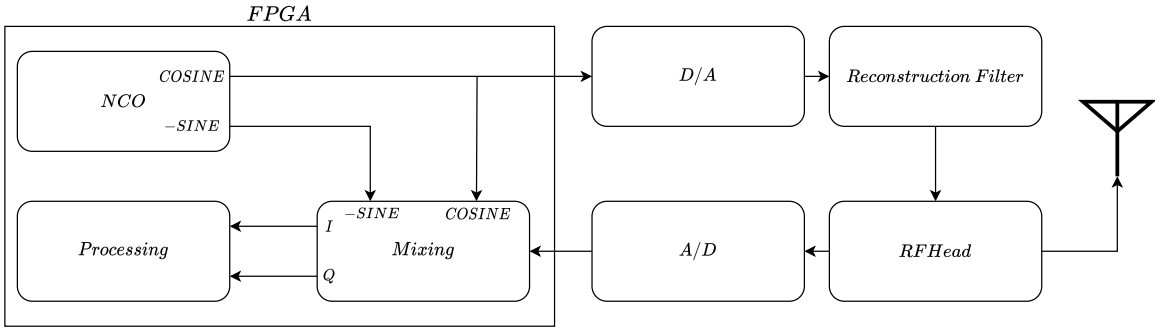

Fig. 2.4: High level diagram of how the I/Q data will be generated

The digital portion of the system will be implemented in a FPGA. The FPGA will house the start and end of the signal chain and contain all but the signal conditioning and sampling. The process starts with a numerically controlled oscillator (NCO) to generate the needed sinusoids. An NCO works by filling a Look-Up Table (LUT) with points of a sinusoid wave. A phase value is used to address the LUT and output the appropriate value to the Digital-to-Analog converter (DAC) which is later filtered. Along with the cosine output signal, a negative sine signal is output for calculations later.

The DAC output is sent through a reconstruction filter. The reconstruction filter is

a low-pass filter (LPF) with a steep cutoff to change the digital stepped sinusoid that is output by the DAC into a smooth sinusoid. This smoothed signal goes to the RF Head and the probe in the plasma. The RF Head consists of a set of transformers that decouple the probe from the loads further down the analog chain that would affect the impedance seen at the probe.

After passing through the probe, an impeded signal is sampled by a high speed ADC. After being sampled by the ADC, the now digital signal is mixed with the original cosine and a negative sine signal. These mixed signals are then low-pass filtered to get the I/Q samples for further processing such as a tracking control loop.

There will be noise present in the I/Q samples that come from sources such as a non-ideal original signal, non-ideal Analog-to-Digital conversion, other instruments on the spacecraft, and so on. Multiple strategies could be employed to improve the inherent noise on the data. Additional filtering to smooth the I/Q sample stream is one method that could be used. Oversampling and averaging would also provide improved samples but more simply. Both oversampling and filtering will be employed for the USU SIP.

This system can meet all of the defined requirements derived from the overall mission requirements. As the individual components were chosen and digital system designed, care was taken to generate samples at the prescribed rates while meeting noise and power requirements.

2.3 SPORT Mission Requirements

The Scintillation Prediction Observation Research Task (SPORT) mission is tasked with answering two science questions:

1. What is the state of the ionosphere that gives rise to the growth of plasma irregularities that extend into and above the F-peak?

2. How are plasma irregularities at satellite altitudes related to the radio scintillations observed passing through these regions?

In order to answer these questions, mission science requirements have been defined. These requirements are given in Table 2.1. These requirements were developed according to the concept of a minimum mission science requirements set, such that if these requirements are achieved then progress can be made on the science questions. These requirements cover what all instruments on the space craft need to accomplish together.

Table 2.1: Top level requirements for the SPORT mission

The Scintillation Prediction Observation Research Task		**Instrumentation**	**Spacecraft**
Observational Approach	Science Measurement Requirements	Instrument Approach	Space System Requirements
1) What is the state of the ionosphere that gives rise to the growth of plasma irregularities that extend into and above the F-peak?			
Observations in the 1700 to 0100 LT sector over -30 to 30 latitude Height profiles of the plasma density to specify the magnitude and height of the F peak density in the EA Vertical ion drifts at or below the F peak in the EA	Plasma Density Profile 1) 140 to 450 km alt 2) 104 to 107 p/cm3 range 3) 20% p/cm3 accuracy 4) 1000 km along track sampling Ion Drifts (Earth Reference Frame) 1) 800 m/s Range 2) 20,m/s precision & accuracy 3) 10 km along track sampling	GPS Occultation Observe GPS satellite occultation along and to the sides of the orbit plane to obtain line of site TEC Ion Velocity Meter Observe vertical ion drifts by angle of arrival of heavy ions at detector	Satellite Orbit 1) 1 year mission life 2) 40 to 55 inclination 3) 350 to 450 km altitude 4) 10 km eccentricity Spacecraft 1) 515 Ram Pointing 1 2) 1 km position knowledge 3) 10 ms timing
2) How are plasma irregularities at satellite altitudes related to the radio scintillations observed passing through these regions?			
Observations in the 2200 to 0200 LT sector over -30 to 30 latitude Observations of irregularities in electron density and E-field power spectral density in slope from 200 km to 200 m	E-Field (Earth Reference Frame) 1) 45,mV/m range 2) 1.1 mV/m precision & accuracy 3) 1 km along track sampling 4) 10 km - 200 m along track waves Plasma Density 1) 103 to 107 p/cm3 range 2) 103 p/cm3 precision & accuracy 3) 1 km along track sampling 4) 10 km - 200 m along track waves B-field 1) 56,000 nT range 2) 100 nT precision and accuracy 3) 1 km along track sampling	E-Field Double Probe Observe probe floating potential for AC E-fields from irregularity GPS Occultation S4 scintillation index Langmuir/Impedance Observe DC and AC probe response for relative and absolute electron density and observe irregularities Three Axis Magnetometer Support VxB computation for ion velocity and E-Field measurements	Spacecraft Mechanisms 1) 0.6 m tip-to-tip booms Attitude (Post Flight Knowledge) 1) 0.05 1-uncertainty

2.4 Plasma Measurement Requirements

The requirements developed for the SPORT mission were used to develop engineering requirements for the Sweeping Impedance Probe (SIP) on the USU Space Weather Instrument. These requirements are given in Table 2.2.

Table 2.2: Derived Requirements for the USU SIP

ID	Description
R1	The Sweeping Impedance Probe (SIP) shall have both Sweeping and Tracking functionality
R2	The SIP shall make measurements in the driving frequency range of 1MHz to 30MHz
R3	A SIP sweep shall consist of 512 measurement steps made at associated driving frequencies
R4	The frequency associated with each step in a SIP sweep shall be reconfigurable during flight
R5	The measurement period for each sweep step shall have a duration of 2.5 ms
R6	A SIP sweep shall be completed within <1.3 seconds
R7	A period of time between the start of SIP sweeps shall be <120 seconds
R8	Tracking mode of the SIP shall produce samples at a 40Hz rate
R9	Tracking mode of the SIP shall track the frequency of the zero phase point of the antenna to within 10kHz
R10	The SIP shall measure phase to within 5 degrees of accuracy
R11	The SIP shall measure impedances in the range of 100Ω to 100kΩ

These requirements reference the two modes that the probe will operate under: Sweeping and Tracking.

2.5 Sweep Function

Requirements R2-R7 reference to the sweeping functionality of the probe. This sweeping measures the magnitude and phase response of the probe over a range of frequencies. This will generate data samples that can be used to generate data sets similar to the set seen in Figure 2.2. This will be achieved by sweeping the output voltage at frequencies from 1MHz to 30MHz (R2) while measuring the impedance of the probe at each frequency. The requirements describe the sweep function to be 512 steps long (R3) and have a duration of 1.28s (R5,R6). The shape of the sweep function will be configurable by programming

a table on the probe. This allows for any type of sweep: linear, triangular, or focused on specific frequencies.

This sweeping function helps to confirm the value of the upper hybrid frequency. The sweeping function will be in addition to the tracking function which is the primary method of measuring the upper hybrid frequency and by extension the plasma density. Because of this secondary nature of the sweeping function, sweeps will only happen once every two minutes (R7).

2.6 Track Function

Whole sweeps are not necessary to calculate the plasma density; only the frequency where the phase of the impedance goes from positive to negative is needed. If this frequency can be tracked, then the plasma density can be calculated at a higher rate for a better sampling of changes in plasma density. Because of this, the tracking mode will be the mode that the SIP operates under most of the time.

Requirements R8-R12 are in direct reference to this tracking mode. The tracking system will implement a control loop that calculates the current phase response of the probe at the current frequency, and then adjust the output frequency accordingly. This control loop will look for and hold at the zero phase point which is the upper hybrid frequency (R9). The resistance of the impedance affects the steepness of the change from inductive to capacitive impedances at the upper hybrid frequency (R10), making it necessary for the control loop to be accurate. In order to meet the science objectives the probe must be accurate to within 5 degrees of the true plasma impedance phase (R11). It also must generate data at a rate of 40Hz to create a detailed enough measurement (R8,12).

CHAPTER 3

ANALOG SYSTEM DESIGN

3.1 Concept of Operations of the Sweeping Impedance Probe Analog System

Figure 3.1 presents a high-level concept of operations of the Sweeping Impedance Probe. The objective of the system is to apply a known voltage to a probe in the plasma, and to measure the current, i, that flows in response to the applied voltage. The current will be detected with an ammeter circuit. The challenge is that the voltage source operates at RF frequencies and the ammeter must measure the vector current, meaning magnitude and phase of the RF signal. Another challenge is to either keep the impedance associated with the voltage source and the ammeter low or to have the impedance be well known. This is so that the voltage across the probe in the plasma is known and that the current flowing in the circuit is not perturbed by the measurement approach. Of the requirements listed in Chapter 2, requirements R2, R9, R10, and R11 are the most pertinent to the analog design.

The general approach is to digitally generate the voltage source, apply the voltage source to the probe, measure the current that goes through the probe, and use the measured current to find the impedance of the probe. A digital source voltage generation is needed for the digital calculation of the impedance. If the voltage source was generated by analog means, more analog components would be needed to sample the voltage source along with the associated current. Because the voltage source is generated digitally a processing chain is needed to smooth out the digital, stepped signal to limit the bandwidth of the signal. If the voltage source is properly generated, the signal spectrum will consist of nearly one single frequency leading to accurate measurements. The full source generation chain consists of an NCO housed on the FPGA, a high speed DAC, and filtering. The source generation was partially moved inside the FPGA by necessity for the digital processing.

Once the voltage source is generated and conditioned it is passed to the probe. The

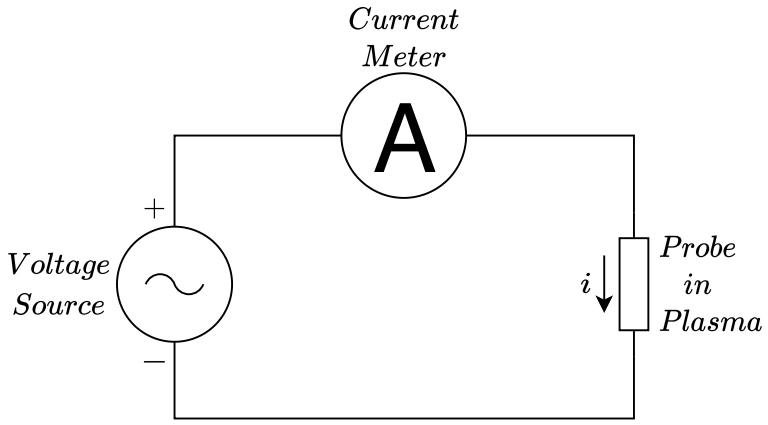

Fig. 3.1: Conceptual diagram of the analog system

probe is isolated between transformers with one of the transformers being a current transformer to convert the current to a voltage for measurement. A high speed ADC then measures this voltage. In the rest of this chapter each of these elements of the impedance probe analog electronics will be discussed and will be generally described. How they are meeting the design requirements will also be discussed.

3.2 Source Generation

To generate the input signal for the probe a narrow-bandwidth voltage signal will need to be created. Secondary frequency content needs to be as small as possible to not affect detection of the upper hybrid frequency. Noise on the signal should be low for the same reason. With these goals in mind, the system seen in Figure 3.2 was used. Full schematics can be found in Appendix A.

In Figure 3.2 the signal flows as follows:

1. A sinusoid is generated by the FPGA using an NCO
2. The digital sinusoid is sent to a high speed digital to analog Converter (HSDAC)
3. The sinusoid is sent through a Low-Pass filter (LPF) to remove high frequencies

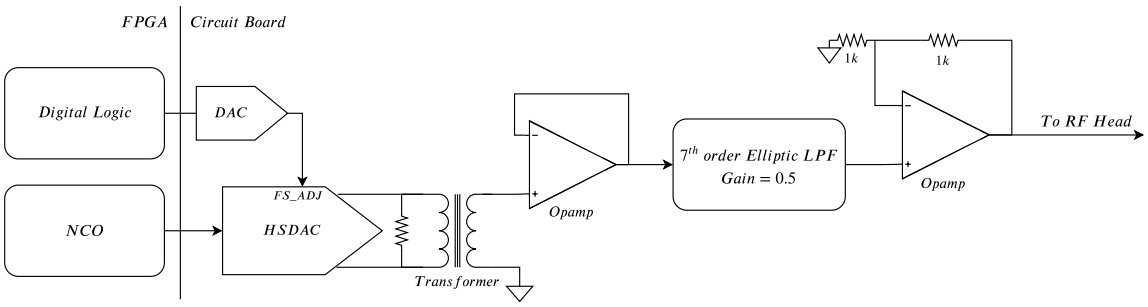

Fig. 3.2: Diagram of the Signal Generation chain for the SIP

This system when implemented properly will generate a very clean single frequency output. The system does have adjustability built in to add further control for a consistent output no matter the frequency being generated. Each portion of this design will be explained in detail here.

3.2.1 NCO Output and High-Speed DAC

As was discussed in Chapter 2 the generation of the output sinusoid starts inside an FPGA. The NCO module outputs a value over a parallel bus to a HSDAC for conversion. The HSDAC used for the USU SIP uses a differential current output instead of a voltage output. By using a differential current output, the HSDAC is able to decrease noise and provide a wider voltage range than single ended DACs [13]. To convert the current output to a voltage, the output currents are passed through a resistor, creating a voltage from the current difference. The value of the resistor used at the output of the HSDAC depends on the desired voltage. If a higher voltage is needed, a larger resistor can be used, or smaller if lower voltages are desired.

The voltage source at this point is stepped because of the digital generation. To remove these steps and the high frequency content that they contain, the signal is next sent into a filtering stage. Along with the data input from the NCO, the HSDAC has a full scale adjust (FS_ADJ) input. This input is used in conjunction with the filtering and will be discussed in section 3.2.2.

3.2.2 Reconstruction Filter

Because the output sinusoid originates from digital synthesis, rather than an analog origin, the output is stepped. These steps bring with them high frequency content. This high frequency content needs to be removed, thus a reconstruction filter is needed. This concept is illustrated in Figure 3.3.

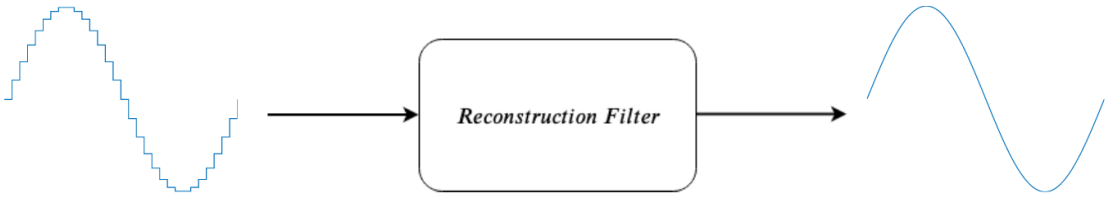

Fig. 3.3: Conceptual diagram of the reconstruction filter

The reconstruction filter was designed under the following requirements:

1. The filter needs to pass frequencies from 1MHz to 30 MHz, to facilitate full sweeping and tracking functionality
2. Frequencies higher than 30MHz need to be filtered out as much as possible
3. The passband gain should be as flat as possible to not affect the magnitude measurement when comparing impedances at different frequencies

These design requirements stem from requirements R2, R9, and R11 presented in Chapter 2. The filter architecture that was selected to fulfill these requirements was a 7th order elliptic filter. Elliptic filters have the highest ratio of passband to stop-band gain but that comes with a trade-off of ripples in both bands [14].

Ripples in the stop-band have a negligible effect on the filter performance as long as the overall stop-band is a sufficient number of dBs lower than the passband. Ripples in the passband, on the other hand, will have a major effect on the accuracy of the impedance measurement. These ripples can be reduced by careful choice of component values in the filter, reducing this problem to an extent. The magnitude and phase response of the designed filter is shown in Figures 3.4 and 3.5, respectively.

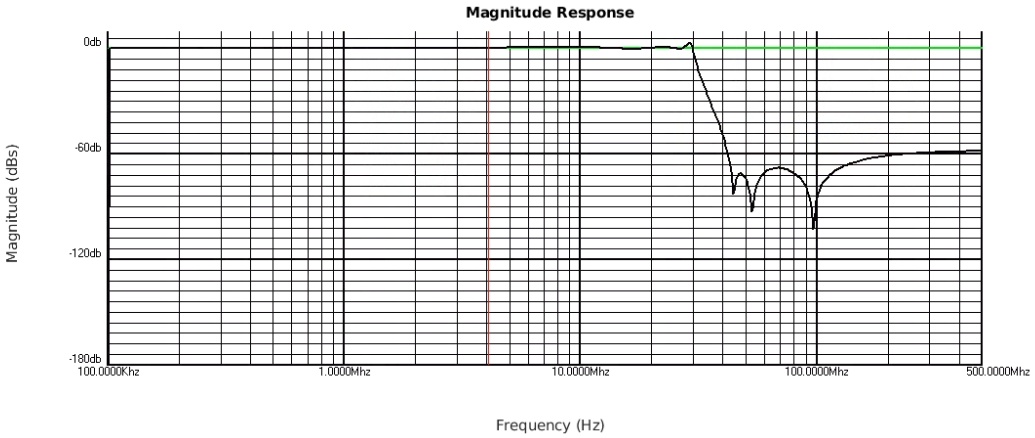

Fig. 3.4: Magnitude Response of the 7th order Elliptic Filter

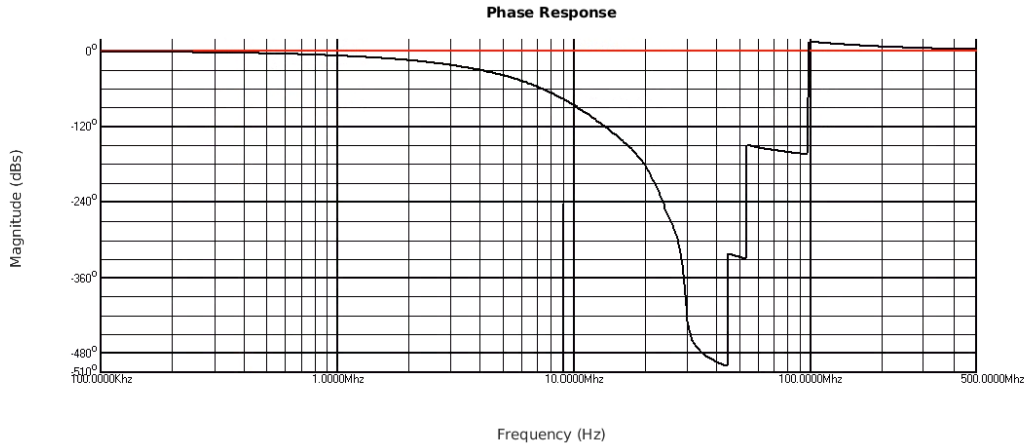

Fig. 3.5: Phase Response of the 7th order Elliptic Filter

Ripples in the passband are still present and need to be addressed to meet the design requirements. The passband magnitude can be flattened by changing the magnitude of the signal going into the filter. Along with the primary HSDAC that outputs the sinusoid, a second DAC is used to control the amplitude of the output signal. The FS_ADJ pin on the HSDAC is used to set the maximum current output from the HSDAC. By using the second DAC, the FS_ADJ pin can be controlled manually, controlling the maximum current output of the HSDAC. During calibration the magnitude of the filter will be measured at different frequencies, and the voltage of the DAC can be set per output frequency to smooth the overall output of the signal generation.

By maintaining the amplitude of the voltage source and filtering out much of the high frequency content, the primary source of variation of the probe excitation is the frequency of the input. This aids in meeting the measurement precision requirements since any variation other than frequency will affect the calculated impedance.

In previous missions, including the ASSP mission, to account for the phase response of the analog system a reference signal was generated. This reference was sent through the same analog components as the measured signal minus the probe itself. This signal then was used to perform the mixing. Because the only phase difference between the two signals was that of the probe, the measured phase offset was accurate. Because the SPORT SIP does all processing digitally, this method would require a second ADC to sample the reference channel. It was decided to not use the reference channel method to avoid the extra power draw that a second ADC would use. The high speed ADC used to sample the probe signal is one of the highest power parts of the entire analog system, so using two of those parts was not possible within the targeted power budget. The digital method to compensate for the analog phase shift is discussed in Chapter 4.

Op-amps are placed before and after the reconstruction filter to decouple the HSDAC output, filter, and loads from each other while maintaining the desired characteristics of each stage. The op-amps were chosen to have sufficiently high gain-bandwidth product, and low enough noise for this application. Lower noise amplifiers could have been used at

the expense of higher power consumption.

3.3 Current Measurement

To measure the impedance of the probe in the plasma the following is needed: to apply the source to the probe with minimal current leaks or other parasitic impedances, and to measure the current with as little noise added in the conditioning as possible. Both are discussed below.

3.3.1 RF Head

Once the generated sinusoid has been filtered it is sent to the probe. The RF Head is the system that applies the voltage source to the probe and protects the current from parasitics that would affect measurement accuracy. The RF Head is made of transformers around the probe connection to aid in isolating the probe effects from any loads or parasitic currents. Figure 3.6 shows a diagram of the probe in the ionospheric plasma and how it fits within the RF Head. In Figure 3.6 the probe component includes the physical probe and the plasma between the probe and the spacecraft. The interaction between the probe, plasma, and spacecraft body was presented in Chapter 2. For this model of the system, the probe and plasma act as an R-L-C circuit. This R-L-C circuit can be analyzed by comparing the voltage and current in the system. As discussed in Chapter 2, if the current can be measured it can be compared to the voltage using the I/Q method to find the response of the probe. To capture the current through the probe and plasma a current transformer is

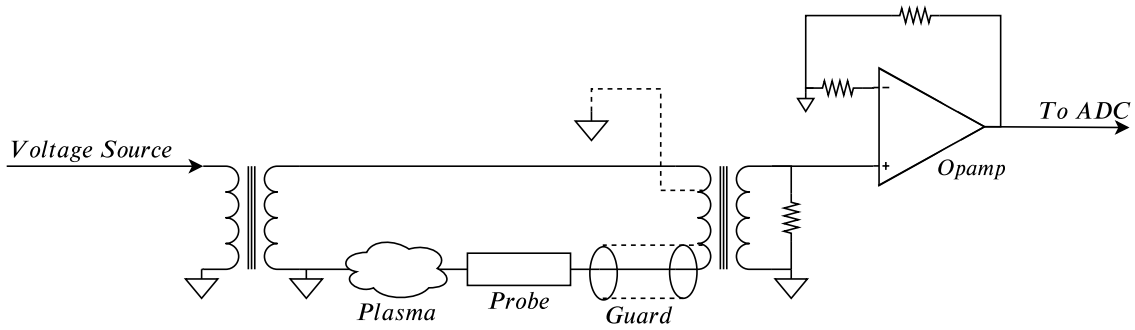

Fig. 3.6: Diagram of the RF Head circuit

used. The current through the probe side of the transformer is converted to a voltage by a load resistor and is then measured by an ADC after being amplified.

Preventing parasitic currents is important for accurate measurements. To prevent any effects on the measurement from these currents, the connection to the probe is guarded. The probe connection is made with shielded wire. The shielding on the wire is grounded to prevent parasitic currents from reaching the current at the probe. To have shielded wire in the transformer, the transformer is hand-wound and attached to the circuit board after fabrication. The guarding aids in meeting requirements R9 and R10.

At the end of this processing chain is a set of op-amps that amplify the voltage out of the current transformer. This gain should be as high as is necessary to reach the full scale input of the ADC. If a signal that is input to the ADC is full scale, the signal will have peak amplitude equal to the maximum voltage that the ADC can measure. All ADCs have an amount of noise inherent in the measurement. This noise is commonly measured in counts in the measurement, where counts is the digital number output by the ADC. By providing a full scale input the number of counts for the signal is much larger than the ADC's measurement noise. This reduces the noise power from the ADC and the overall noise in the measurement.

3.3.2 Sampling

The final step of the analog system is to sample the data coming from the RF Head. A diagram of the sampling system is shown in Figure 3.7. The sampling is done with a High Speed ADC (HSADC). To sample with little noise, a differential ADC is used.

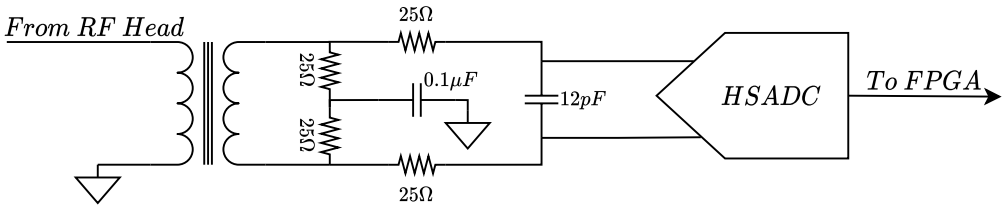

Fig. 3.7: Schematic of Sampling System

Using a differential ADC requires that the signal to be sampled is encoded in the voltage difference between two input lines. To create this differential signal the circuit in Figure 3.7 is used. This circuit is the suggested method from the data sheet of the HSADC used in the design [15]. For data transmission between the ADC and the FPGA, a parallel bus is used to meet sample rate requirements.

CHAPTER 4

DIGITAL SYSTEM DESIGN

To control all the needed functionality of the SIP, the digital system was designed as shown in Figure 4.1. Figure 4.1 flows generally from left to right for the system control and right to left for measurement handling and processing. All major subsystems seen in the design are detailed later in the chapter. The detailed figures retain the same data flow directions for comparison to Figure 4.1.

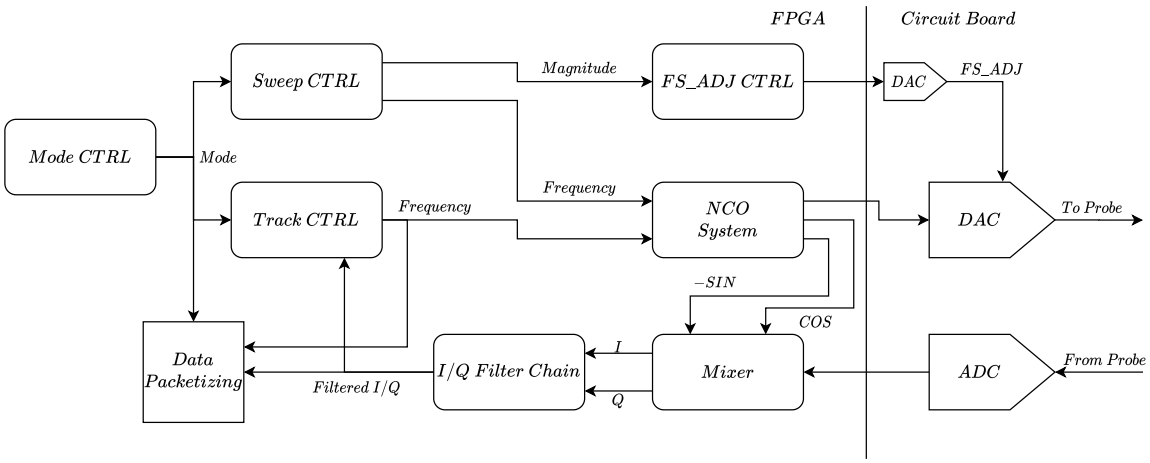

Fig. 4.1: Top Level Diagram Digital System

The system starts with the Mode Control block which toggles between Sweep and Track mode. The output mode control signal is then fed to the major control blocks. Each major control block, when enabled, manages the whole probe and set how the data measurements are organized for packet outputs. Once the mode is set, the mode control blocks will manage what signal is output to the probe. The Mode Control takes inputs from the microprocessor to determine which of the modes to be in, or to alternate. If alternating between modes, the Mode Control will time when the switch will happen (R7).

The Sweep Control subsystem will output a predefined frequency sweep, via the NCO,

measuring the probe impedance in a frequency range of 1-30MHz. The magnitude of the output of the FS_ADJ DAC is also controlled at each step of the sweep. This provides a constant amplitude signal to the probe to such that any magnitude change on the measurements is only from the probe and not from the other analog components. This subsystem does not require any external inputs while enabled.

The Track Control subsystem tracks the upper-hybrid frequency of the ionospheric plasma discussed in Chapter 2. To do this the subsystem receives the filtered I and Q from the probe and calculates the phase of the probe impedance. At the upper hybrid frequency the phase equals zero, providing a simple point to track. Using a control loop with the calculated phase as the input, an output frequency is generated to track the desired frequency. This generated frequency is sent to the NCO for output and is the data that is packetized for tracking packets.

The data input from the ADC is first mixed to generate the I and Q data that is then low-pass filtered and accumulated for use. In sweeping mode the I and Q data is sent directly out as the sweep data, while the track uses the I and Q data to calculate the phase offset. The data packetizing consists of gathering the needed data for one granule of the full packet then handing of the data to the on board microprocessor to build the complete packets.

The HDL for the system was written in VHDL using state machine style behavioral design for all controllers while the data processing chain was written as RTL design. The full development project with all the FPGA HDL and microprocessor C code is included in Appendix A.

4.1 Signal Generation

The output signal generation system is shown in Figure 4.2. This system outputs the proper frequency of sinusoid and accounts for the analog system response through which the signal will pass. By accounting for the analog system response, the impedance of the probe in the plasma can be isolated.

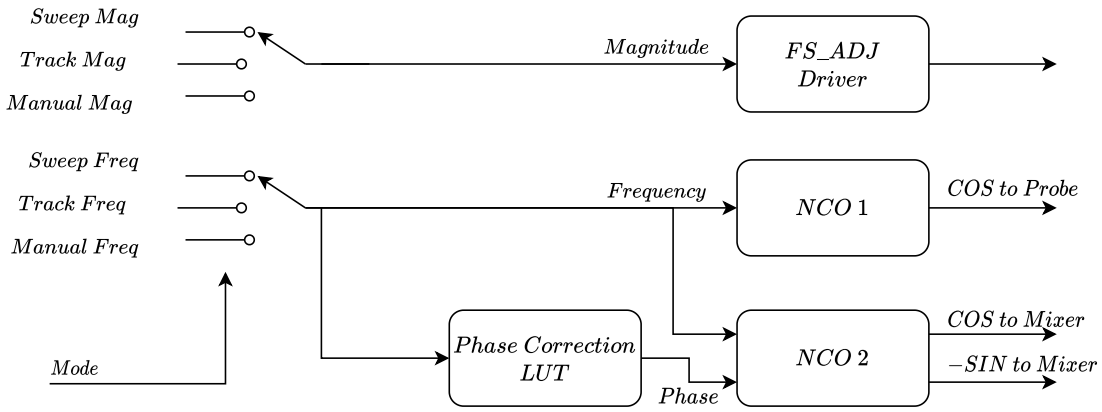

Fig. 4.2: NCO and FS_ADJ System

To fully account for the system response of the analog system, both magnitude and phase of the output has to be adjustable. By using the FS_ADJ output and two NCO blocks, both the magnitude and phase response of the analog system can be compensated for. For details on the response of the analog system see Chapter 3.

To generate the signal that goes out to the probe, NCO 1 and the FS_ADJ driver output to the two DACs. The NCO controls the frequency of the outgoing signal while the FS_ADJ controls the magnitude of the signal. To create a sinusoid wave the NCO contains a LUT that is loaded with one period of a sine wave that is then referenced for the output. To decide which entry in the table to use, the NCO contains a register that holds the phase offset of the signal. Every clock cycle the NCO will increment the phase register, reference the table at that phase, then output the data stored in the table. To adjust the frequency of the output sinusoid the amount the phase is incremented by is input to the NCO. This adjustable phase increment gives the NCO an output range of 0Hz to $0.5f$ where f is the frequency of the NCO clock. The NCO clock for the USU SIP is set at 80MHz, giving a possible output frequency range of 0Hz to 40MHz. For more information about the theory of NCO operation, and specifics about the NCO used in this project, see [16].

The phase correction process was simulated using Simulink and multiple correction methods were implemented and tested to determine what methods would best meet the

requirements. All of the methods were based on lookup tables to correct for the known and potential timing and phase delays within the system. The methods attempted included correcting for the phase delays after the mixing by converting I and Q samples into magnitude and phase and then adjusting the phase using a LUT. Attempts were also made to adjust the I and Q samples directly using a LUT. All of these methods suffered from resolution problems in that the phase could not be reasonably corrected given the bit size of the digital words used to represent I, Q or magnitude and phase.

The method that was determined to be the most useful was to adjust the phase of the numerically controlled local oscillators as a function of operating frequency. The outputs from NCO 2, the local oscillator, are generated for the purpose of mixing with the measured signal. In Chapter 2 the theory of the mixing operation was presented. In that discussion it was shown that the mixing operation finds the magnitude and phase difference between the input signal and the mixed signal, presented in rectangular form. If the phase difference is what is found, the reference can be adjusted to remove any phase change due to the analog chain. The resolution of the phase accumulating register for the NCO is such that phase delays can be potentially controlled down to the 10 micro radian level giving precise control of phase corrections for the system.

The response of the analog system, including the reconstruction filter, was estimated by simulation and verified in calibration. A resistive load, which should produce a zero-phase delay in the measurement, is used for calibration. The correction phase offset table is constructed from the measurement of the resistive load across the frequency range of the instrument using a zero lookup table. The observed phase delay becomes the needed phase offset that is subtracted from the phase of the mixing local oscillator. By subtracting this expected change with the mixing signal the only phase difference remaining in the system is the phase change caused by the probe in the ionospheric plasma.

To adjust the phase of the mixing signals a 16-bit phase LUT is used. This table takes the current output frequency as the input. Using the current frequency, a phase adjustment is determined and sent to NCO 2. This phase offset will make the outputs from the two

NCOs the same signal aside from the shifted phase of NCO 2. To assure that the NCOs maintain this sameness of output, the NCOs will be synced at each mode change.

In order to generate the appropriate signal for each mode of operation, three-way switches are put in front of the system. These switches are controlled by the mode controller. They also give the option of manual control for calibration.

4.2 Signal Reception and Processing

The reception of the returning sinusoid is processed in the following order: ADC sample, mix, accumulate, LPF, accumulate, then packetize. This process is detailed in Figure 4.3.

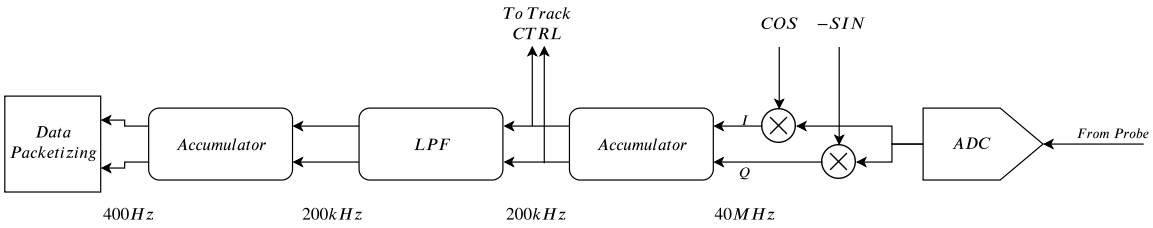

Fig. 4.3: Signal Reception and Processing Chain

The final measurements of I and Q are produced at a rate of 400Hz. In the sweeping mode the frequency is adjusted between samples. Given that the initial production of I and Q samples is at 40MHz, the system is oversampling by a factor of 100,000. Averaging and filtering are used to reduce the sampled data rate and also decrease the noise within the samples, increasing the precision of the measurement. As long as the noise power in the sampled signal is at least one ADC bit then oversampling techniques can be used to increase the resolution of the measurement. By coupling the oversampling with the needed math operations, mixing and filtering, data of high enough quality for the system requirements can be measured.

The 14-bit ADC will sample at a 40MHz rate. For the driving frequencies above 20MHz an aliased frequency will be produced and the resultant signal will be folded back into the 20MHz bandwidth. The magnitude and phase of this aliased signal can still be determined so that aliasing is not an issue with this signal in measuring frequencies in the 20MHz to

30MHz range.

The filtering and accumulating functions increase the number of bits needed to represent the samples similar to the operation of a delta-sigma ADC. As a general guideline, oversampling by a factor of four provides one additional bit of resolution in the sampled signal. Thus, an additional 8.3 bits of resolution should be provided by the oversampling of I and Q by 10^5. The resultant 20-bit values of I and Q from the 14-bit ADC with an additional 8 bits of oversampling should be nearly noise free.

4.3 Sweep Control

The sweeping system needs to output a range of frequencies to the NCO, then for the input to be sampled. To control this, the system in Figure 4.4 is used. The frequencies to be output are stored in a LUT of frequency values for the NCO. There is also a LUT for the FS_ADJ magnitude. The values in the FS_ADJ LUT correspond to the frequency at the same address in the frequency table. The outputs from each of the tables are sent out to create the desired signal. The controller simply increments the address for the tables to output. The controller also controls the timing of the address steps. When disabled by the mode controller, the sweep controller resets and waits to be enabled at the next sweep.

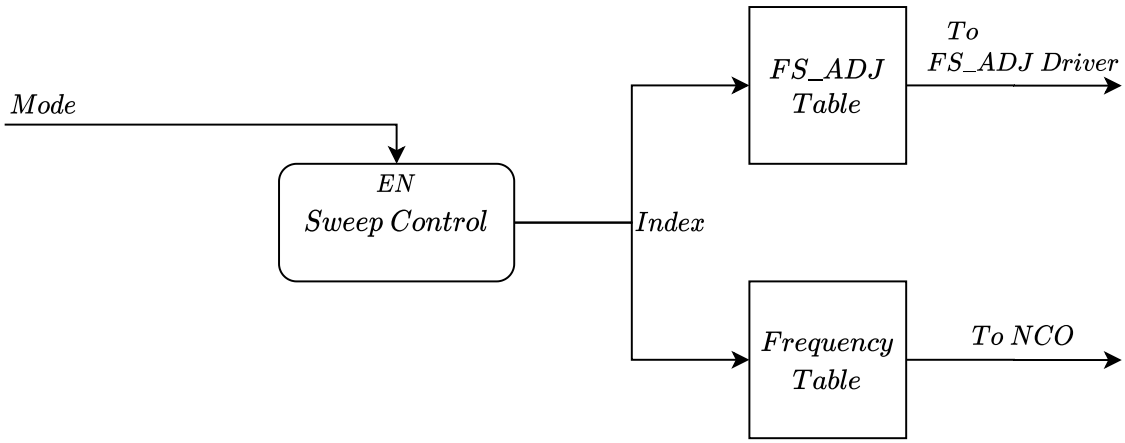

Fig. 4.4: Sweep Control System

4.4 Track Control

The goal of the tracking system is to find the upper hybrid frequency and track it as the spacecraft passes through the ionosphere. Figure 2.2 shows the type of impedance response expected at the probe. Since the probe is measuring current the probe will have negated phase from what is seen in the figure. The upper hybrid frequency is the frequency where the phase response goes from inductive to capacitive, i.e. negative to positive. Normally a Proportional-Integral-Differential (PID) controller would be used in this type of situation, but because of the simple negative-to-positive nature of the response a simple gain can be used for tracking. If the measured phase is positive the output frequency needs to be lower; if the measured phase is negative the frequency needs to be higher. Figure 2.2 also shows that at lower frequencies the phase is capacitive. To avoid this area, limiters are built into the system to prevent the frequency from going too low and crossing into that range.

To accomplish the tracking, the control loop needs to calculate the measured phase, adjust the output frequency according the phase, and limit the frequency to avoid the low frequency capacitive region of the response. To do this, the system in Figure 4.5 is used.

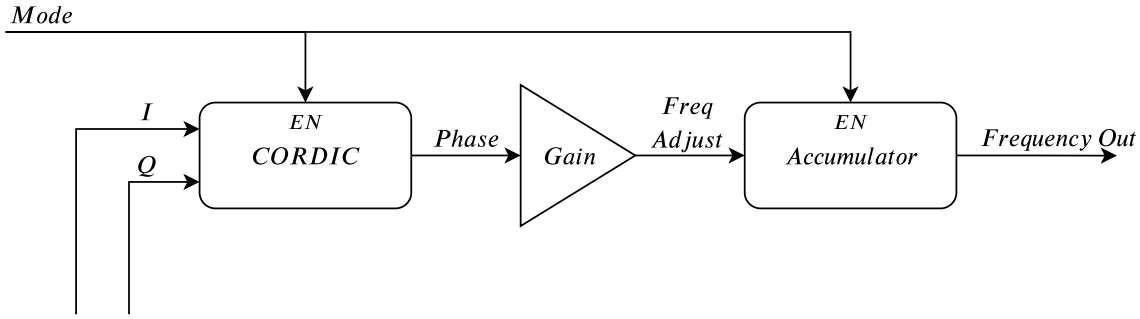

Fig. 4.5: Tracking Control Loop

First, the measured I/Q samples are brought into the loop and into a Coordinate Rotation Digital Computer (CORDIC). A CORDIC is used to digitally calculate trigonometric operations such as the inverse tangent needed to find the phase between the I/Q values.

Once the phase has been calculated it is converted into a frequency adjustment by using a gain. This gain will be approximately $-0.1/\pi$ counts/degree(rad). This gives a conversion

from radial frequency to a frequency adjustment. This gain is implemented using bit shifts and a negative accumulation for simplicity. The gain of $-0.1/\pi \approx 5$ right bit shifts, and $-0.05/\pi \approx 6$ bit shifts and so on. The system allows from one to seven shifts which gives a gain range of $-1.6/\pi$ to $-0.025/\pi$. Tuning this gain will balance how fast the system can find the zero phase point with how accurate the tracking is. The gain is configurable on flight.

After being calculated, the frequency adjust is accumulated into the frequency output. The accumulator will monitor the current frequency to check for too high and too low frequencies. If the frequency in the accumulator is either too high ($>$ 28MHz) or too low ($<$ 3MHz) it will reset to a central frequency of 6MHz. This prevents the output from going into frequencies that have undesirable phase responses. This frequency is sent to the NCOs for signal generation.

Like the other subsystems, the tracking loop is disabled when not in use.

4.5 Data Handling and Transmission

The data from the USU Space Weather Instrument are in packet formats with different packets for each type of measurement as well as a few other system packets. All system packets with their full structures are thoroughly defined in [17]. For this document, only individual granules from the SIP Sweep Packet and SIP Track Packet will be discussed. A granule from each of these packets represents one data sample. The lager packets contain multiple of these granules. By having multiple granules in each packet the amount of data overhead is significantly reduced. The granule structures for the SIP Sweep Packet and the SIP Track Packet are given in Figures 4.6 and 4.7, respectively.

Word Number	Bit Number															
	15	14	13	12	11	10	9	8	7	6	5	4	3	2	1	0
1	SIP I (MSB 16 bit)															
2	SIP Q (MSB 16 bit)															
3	SIP Q (LSB 4 bit)				SIP I (LSB 4 bit)				NO DATA							

Fig. 4.6: Granule Structure of the SIP Sweep Packet

Word Number	Bit Number															
	15	14	13	12	11	10	9	8	7	6	5	4	3	2	1	0
1	SIP Track (MSB 16 bit)															
2	Blank		SIP Track (LSB 14 bit)													

Fig. 4.7: Granule Structure of the SIP Track Packet

The SIP Sweep Packet contains a 20-bit representation of each of the I/Q samples. Similarly, the SIP Track Packet contains the 28-bit value representing the phase offset sent to the NCO to track the upper hybrid frequency. Along with a number of these granules, each full packet also has a timestamp of when the data was generated, a header, and checksum.

To get the data from the FPGA into packets for downlinking, the process shown in Figure 4.8 is used.

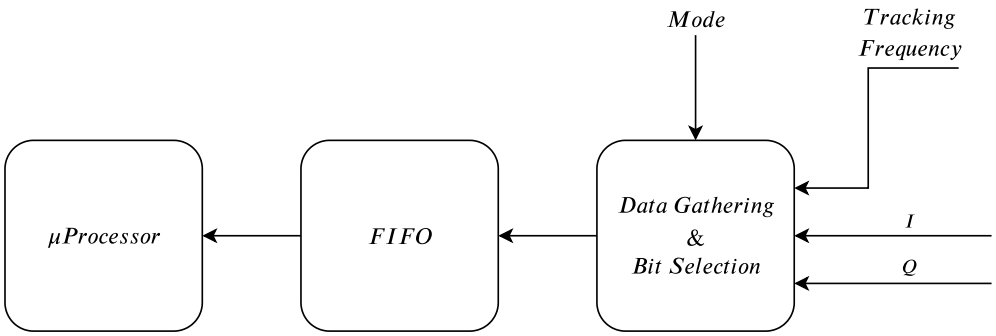

Fig. 4.8: Data Flow of the Data Packetization

The data is first gathered from the other subsystems and the desired bits are selected from those samples. In sweeping mode there is a chance that the I and Q data will not arrive at the same time, so the Data Packetizing block will always wait for both samples to arrive before writing them to the FIFO.

The FIFO (First-In, First-Out) is a memory buffer used to bridge the divide between the FPGA fabric and the microprocessor. There a few reasons the data needs to be buffered. First, the processor and FPGA use different clocks making passing signals between the

two more complicated than within just one of them. Second, the processor is tasked with handling many other data streams and can only process one stream at a time. It is unknown when the processor will get to the SIP system for data reception. The FPGA will be continuously generating data so there needs to be a buffer separating them.

If there is data ready the microprocessor will be flagged by the FIFO. This data is read from the FIFO and put into a packet. Once the processor has enough granules for a whole packet, a header and checksum are added. This finished packet is held until it gets read from the host managing the USU Space Weather Probe.

CHAPTER 5

TESTING AND VERIFICATION

The testing of the SIP is to verify the compliance of the instrument with the requirements presented in Table 2.2. A number of methods are employed to verify the requirements including verification by design of the instrument, through analysis, through functional testing and though specific calibration test procedures. Table 5.1 presents how each of the requirements are verified.

Table 5.1: Testing needs to meet requirements

ID	**Description**	**Verification Method**
R1	Both Sweeping and Tracking Functionality	By Design
R2	Frequency output range of 1MHz to 30MHz	By Design and Functional Testing
R3	512 Sweep measurement steps	By Design
R4	Reconfigurable during flight	By Design and Functional Testing
R5	2.5ms Integration period per step	By Design
R6	1.3 seconds per sweep	By Design and Functional Testing
R7	120 Seconds between sweeps	By Design and Functional Testing
R8	Tracking rate $\geq$40Hz	By Design and Calibration Testing
R9	Find and track the frequency of the zero phase point to within 10kHz	By Calibration Testing
R10	Measure phase to within 5 degrees of accuracy	By Calibration Testing
R11	Measure impedances in the range of 100$\Omega$to 100kΩ	By Calibration Testing

Of the testing verifications listed, all that are in regards to timing, sample rates, and sweep steps and system modes are based in the digital design of the SIP. These requirements were tested throughout development of the digital portion of the system and do not need any specialized testing procedures.

Verification of requirements R2, R4, R6, R7, R9-R11 do require testing to confirm

compliance. These will be performed during system calibration. During calibration any offsets and non-linearities inherent in the system can be found and compensated for. By performing this calibration, compliance to the requirements can be confirmed.

The other verifications, R1-R9, are implemented in firmware and will also be verified by analyzing the firmware design.

5.1 Calibration Hardware

To calibrate the system, external calibration loads will be used to stimulate the instrument. The calibration loads are purely resistive, purely capacitive, purely inductive and tuned R-L-C circuits. In Chapter 3, the probe in the plasma was described as having electrical characteristics similar to an R-L-C circuit. The tuned circuit calibrators are built to this model and are used to calibrate the tracking probe. To insert the calibrator in place of the ionospheric plasma the probe used by the system was designed to accept a load via an SMB connector. This way the calibrator can be directly connected to the system to model the plasma using the same electrical path. Figures 5.1 and 5.2 show the two calibrator designs.

The Type 1 calibrators, seen in Figure 5.1, were built to do individual resistive, capacitive, and inductive testing. The Type 2 calibrators, seen in Figure 5.2, were built for resonant testing.

Using Figure 3.6 as a guide, the calibrators will replace the ionospheric plasma in the circuit. The J2 connector on the calibrator will connect to both the primary signal line and the signal guard to properly replicate the probe and maintain the signal protecting properties included in the design. The J1 connector will connect directly to the main system ground as seen in Figure 3.6.

Once the calibrators were built they were tested using a network analyzer to document the true characteristics of the calibrators so when they are attached to the SIP the recorded data can be correlated to the true measured value. Details of the exact resistor, inductor, and capacitor values used in the calibrators along with the characteristics of the calibrators used are in the detailed testing report found in Appendix A.

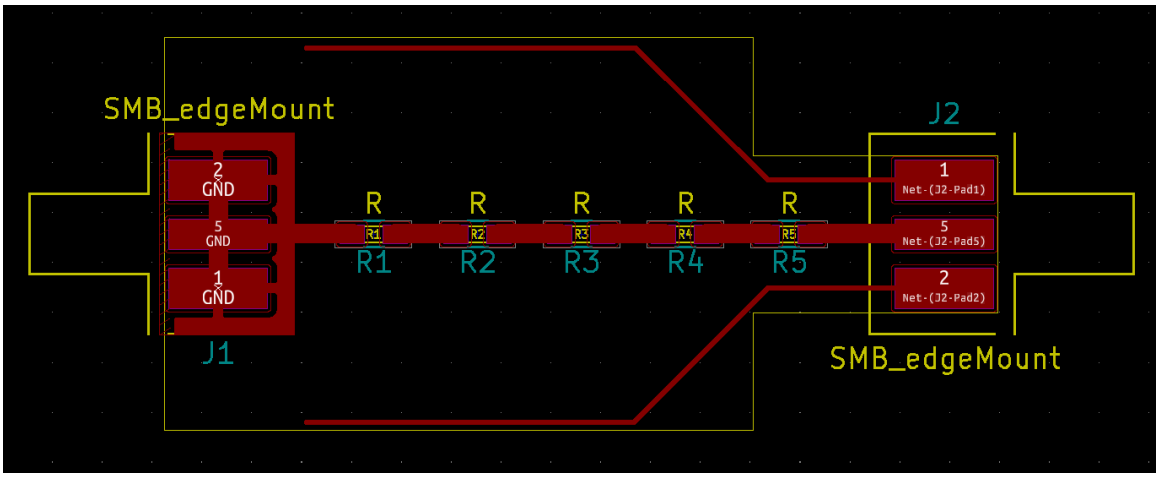

Fig. 5.1: Type 1 Calibrator

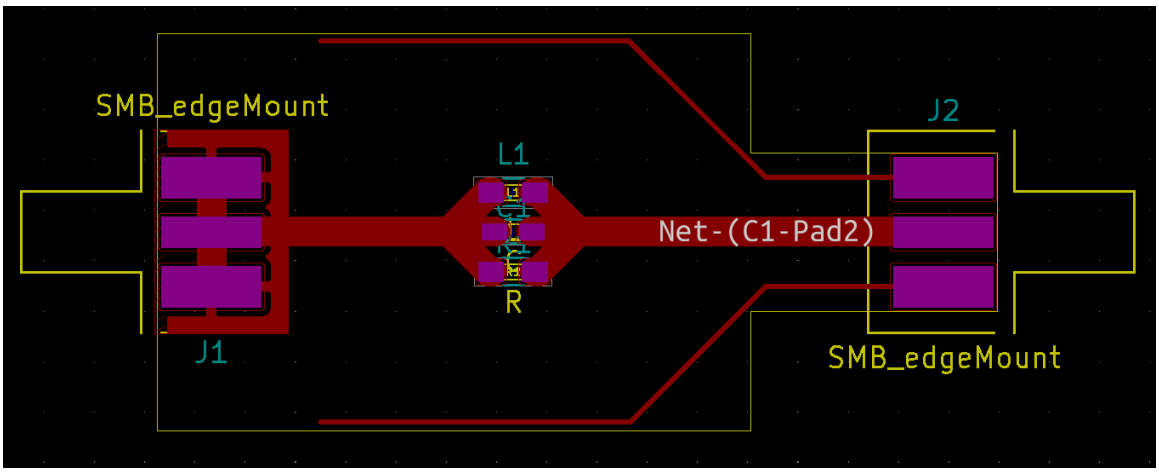

Fig. 5.2: Type 2 Calibrator

Testing and Calibration The calibration testing procedures consisted of the folowing four types:

1. Frequency Output Test
2. Precision, Gain, and Linearity Test
3. Frequency Response Test
4. Frequency Lock Test

During the course of testing calibration will also be performed. This calibration will determine the magnitude and phase response of the system without loading from the probe. All the testing steps will be discussed with a sampling of test data provided.

5.1.1 Frequency Output Testing

Both Sweeping and Tracking modes require a controllable output frequency from the HSDAC. It is required that this frequency can range from 1MHz to 30MHz (R2) and has 512 output steps (R3). The output frequency needs to be precise and have few spurious frequencies.

This test can be performed with an oscilloscope that has Fast-Fourier Transform (FFT) functionality or similar method. The SIP will be set to output a set of frequencies in the operating range and measured by the oscilloscope. The FFT generated from the measured output of the HSDAC can then be analyzed to see if the output frequency is as expected and if there are other spurious frequencies present in the signal. Figures 5.3 and 5.4 show FFT outputs from one such test.

In Figure 5.3and 5.4 the grid marks 5Mhz change in the x-direction and 20dB change in the y-direction. Looking at Figure 5.3, the desired output frequency of 10MHz is seen as the highest point on the plot. The next most powerful frequency is at 30MHz, but it is approximately 30 dB down making the spurious frequencies acceptably low powered. This signal will also be filtered to aid in isolating the desired frequency.

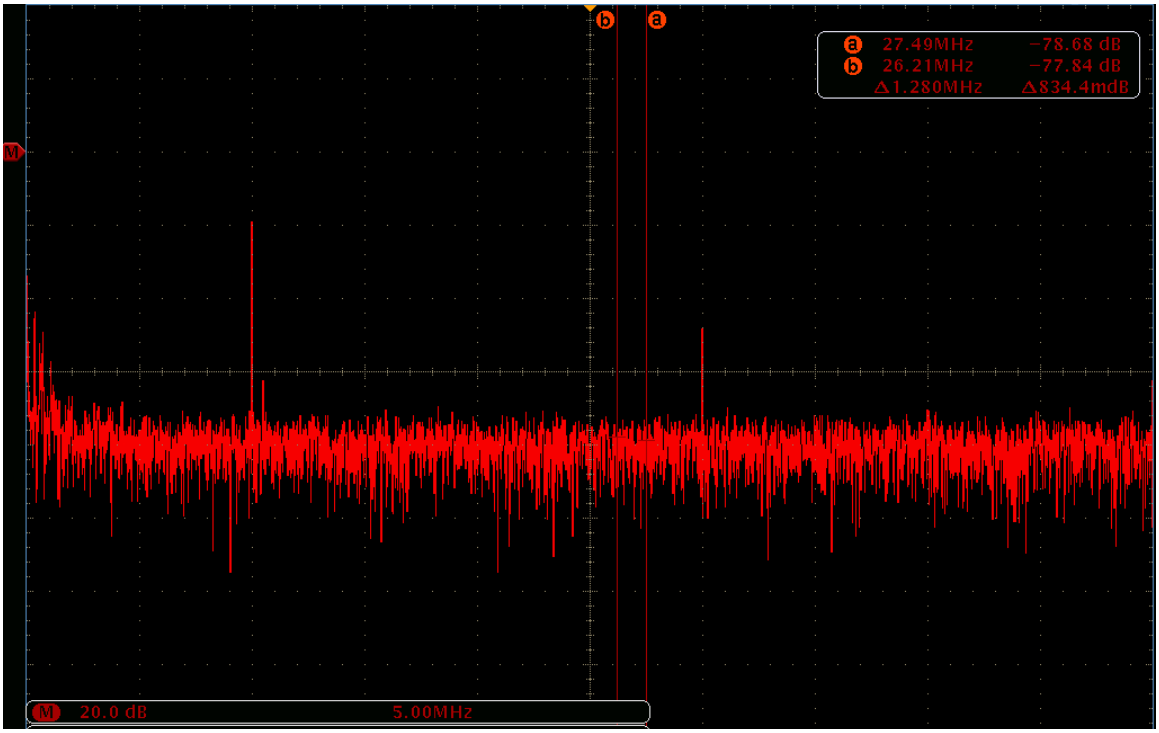

Fig. 5.3: FFT of 10MHz Voltage Source

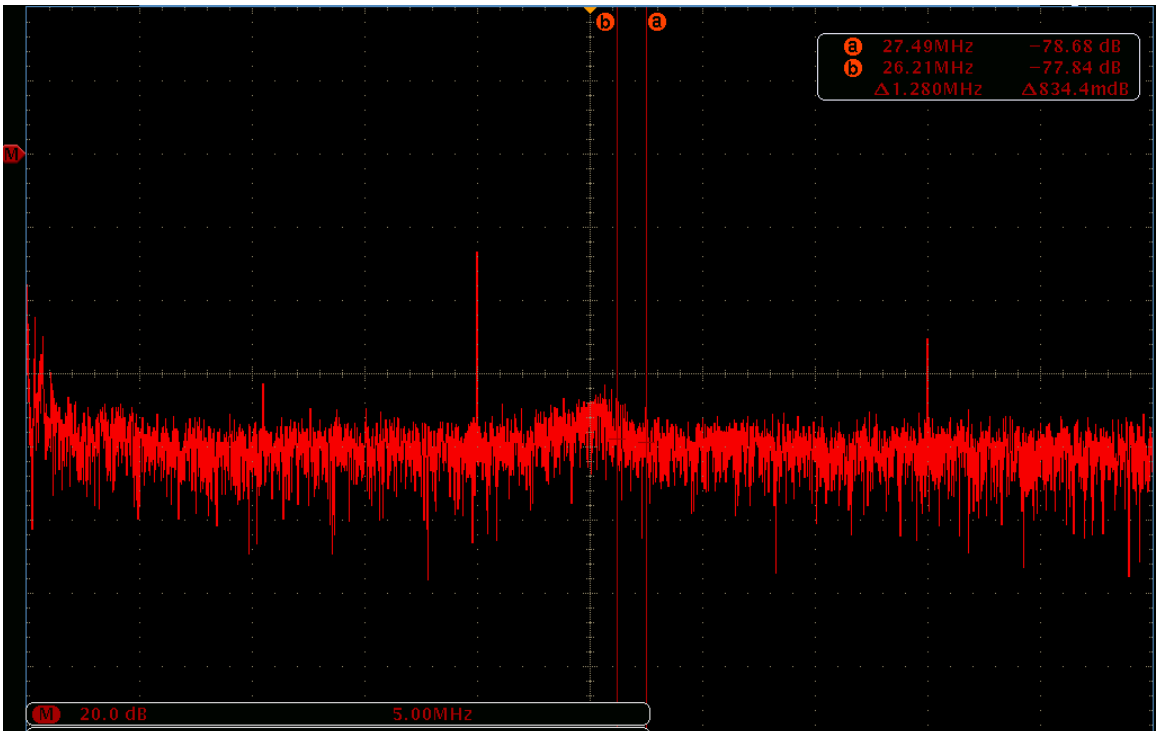

Fig. 5.4: FFT of 20MHz Voltage Source

5.1.2 Precision, Gain, and Linearity Testing

The analog system will contain most of the system effects that require calibration. Within the analog system the areas that will be focused on are the system precision, gain, and linearity. Precision is in reference to how much noise is within the analog chain. This noise can come from all of the analog parts with resistors, opamps, DACs/ADCs, and parasitics contributing the bulk of the noise. This noise will be measured as a whole by determining the noise power in the measured data.

To correlate the measurements accurately to voltage inputs and then to current through the probe, the gain of the system needs to be modeled. Gain testing is testing for both, accuracy of the gain, and to see if the gain is linear across the full range of inputs. Even if the gain is not completely linear, the measured gain curve can be used to adjust the measurements to account for non-linearities.

5.1.3 Frequency Response Testing

It is required that the SIP measure impedance phase to within five degrees of accuracy (R10) and measure impedance magnitude from 100Ω to 100kΩ (R11). After the analog system has been tested and calibrated, the probe measurements should match the true response of each calibration load. This test consists of using the calibration hardware and sweeping across the frequency range of the SIP and measuring the impedance. This will confirm the range of measurable impedances and accuracy of the measurements. Any deviation from the expected measurements can then be recorded as the response of the SIP system itself and can be used as calibration data for future tests. Figures 5.5 - 5.8 show a series of response tests that were performed after calibration tables had been filled.

In Figures 5.5 - 5.8 magnitude and phase data of resistive, capacitive, inductive, and R-L-C loads are shown. Note that after calibration the phase of the resistive, capacitive, and inductive tests is approximately 0, 90, and -90 degrees, respectively. As evidenced by only primarily 0 or ±90 degrees of phase, the calibration of the system to account for the system response is working. When the R-L-C tuned loads are used, as in Figure 5.8, the response has the expected shape having smooth transitions from inductive to capacitive

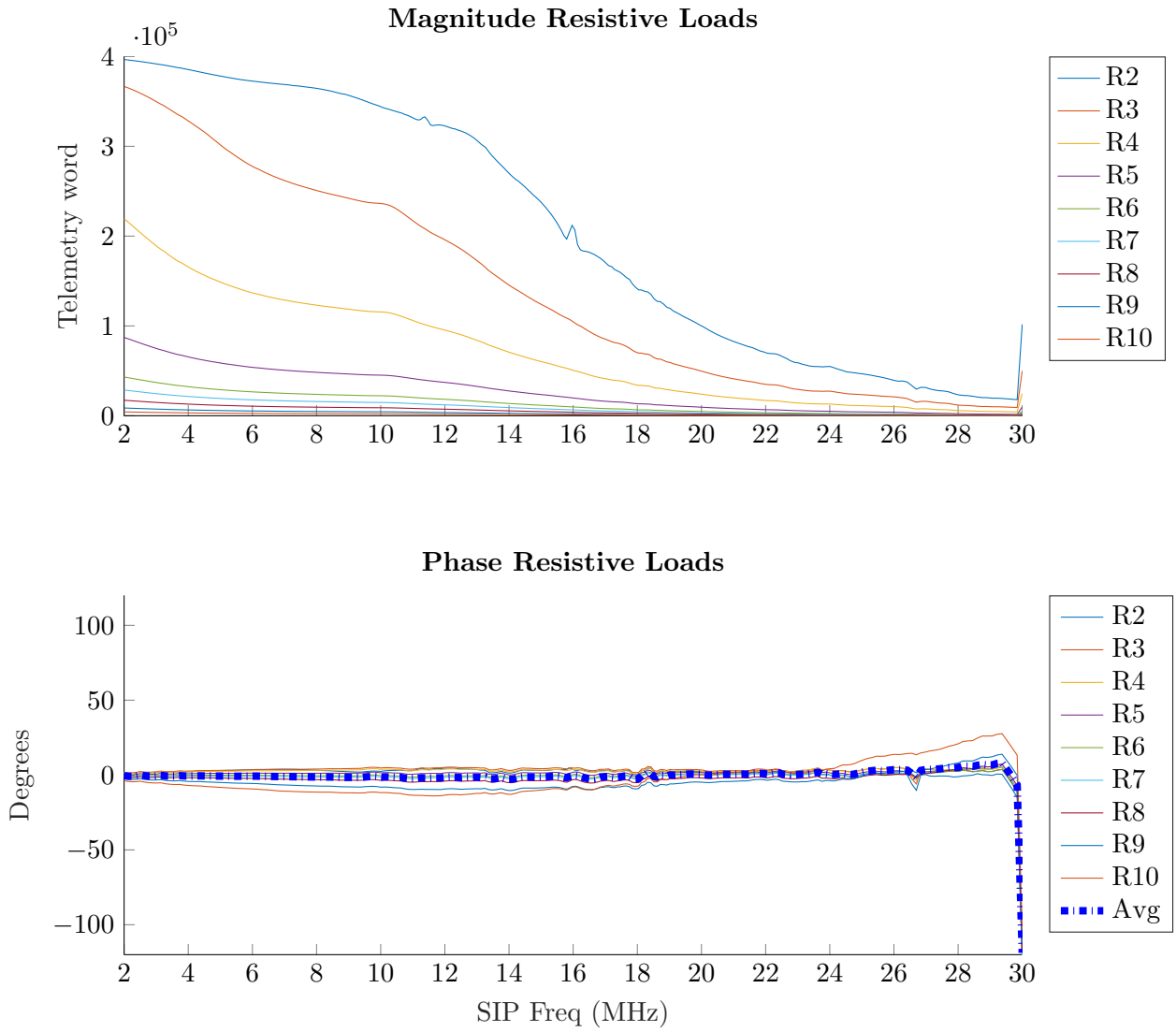

Fig. 5.5: Response of Resistive Load

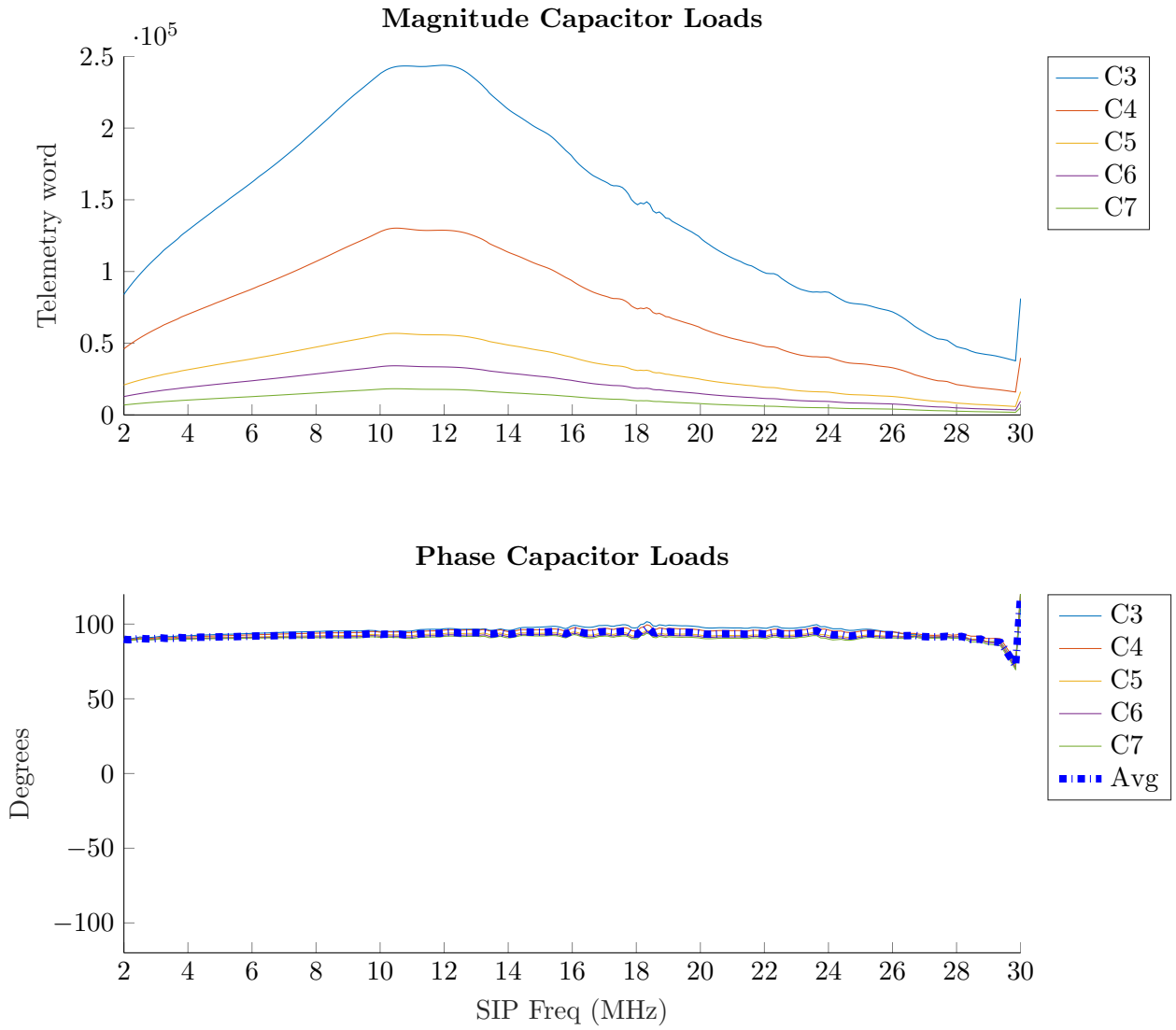

Fig. 5.6: Response of Capacitive Load

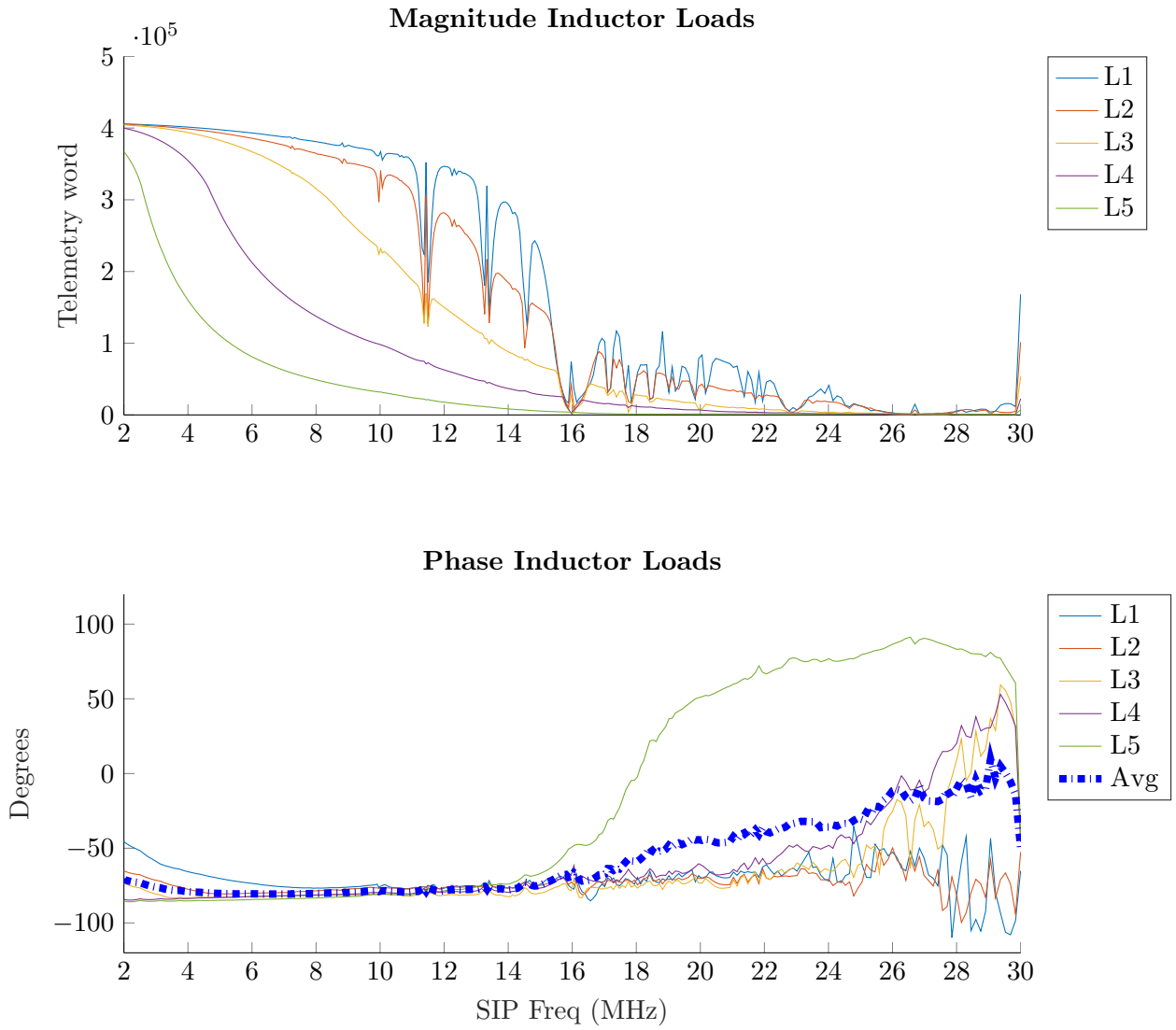

Fig. 5.7: Response of Inductive Load

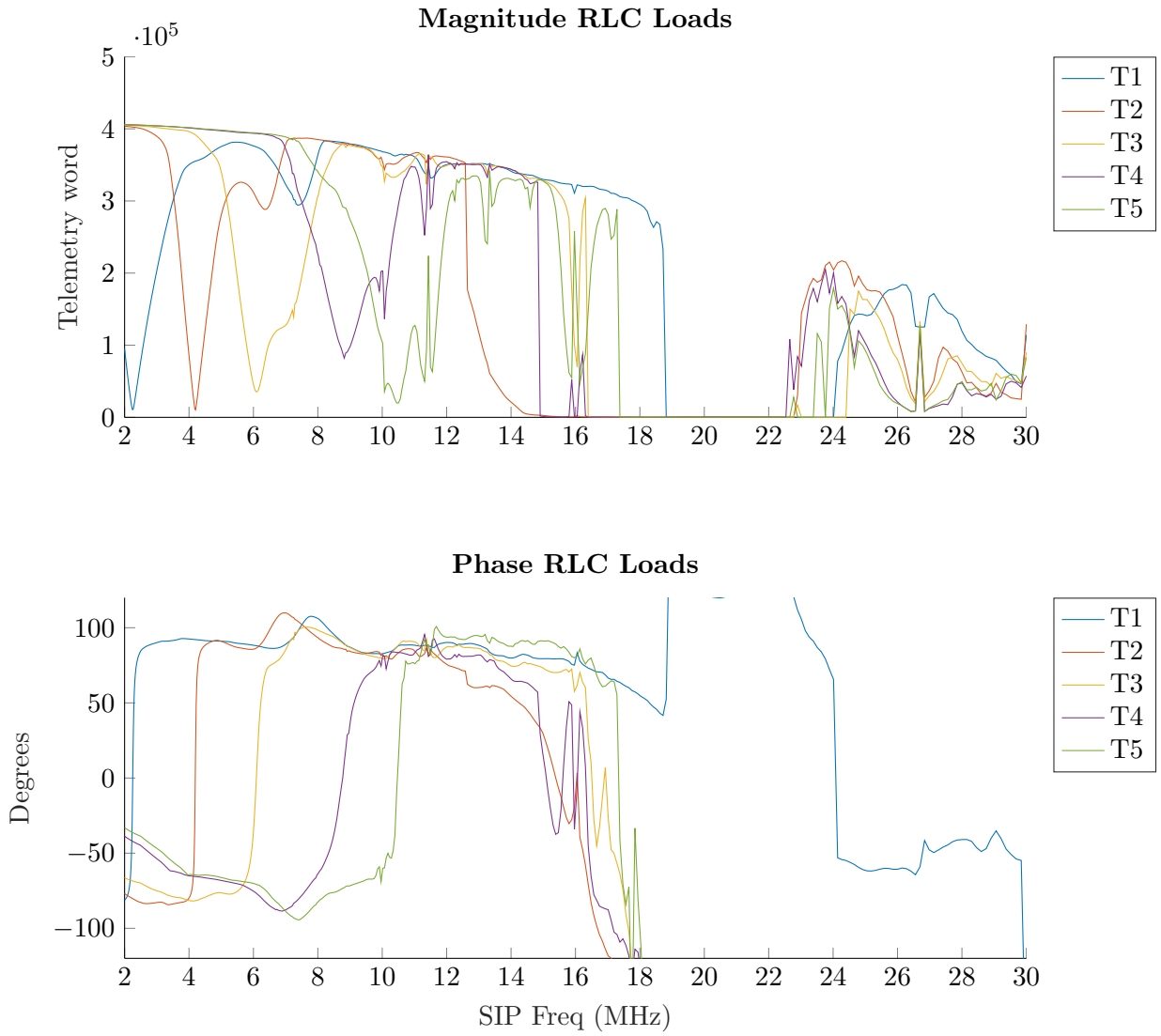

Fig. 5.8: Response of Tuned Load

phase. These transitions also meet the accuracy requirements (R9, R10).

5.1.4 Frequency Lock Testing

The Tracking mode of the SIP is required to determine, and track, the Upper Hybrid Frequency to within 10kHz (R9). This is directly tied to the SIPs ability to measure and calculate accurate phase values. The requirement for phase measurement is to be accurate to within 5 degrees (R10). These requirements will be met by reducing parasitics in the analog processing chain, and by having accurate calibration data. By testing with known loads any offsets can be found and accounted for in the processing chain. The digital system includes the tables needed for storing and using these calibrations.

The Frequency Lock Testing can be done once a satisfactory calibration table has been created and loaded. Figure 5.9 shows an output of the tracking system. The figure shows the tracking output for seven tracking sessions with a sweep happening every 2 seconds. The sweeps show up in the tracking data as unchanging times in the data. It can be seen that the tracking finds and holds on a frequency of 4.12MHz which is accurate for the T2 calibrator.

5.2 Testing Conclusion

The engineering requirements given at the start of this chapter were derived from the overall science requirements of the SPORT mission. If these engineering requirements are met then the SIP will be capable of meeting the mission science requirements.

After performing the tests outlined in this chapter, the SIP was found to meet all of the engineering requirements.

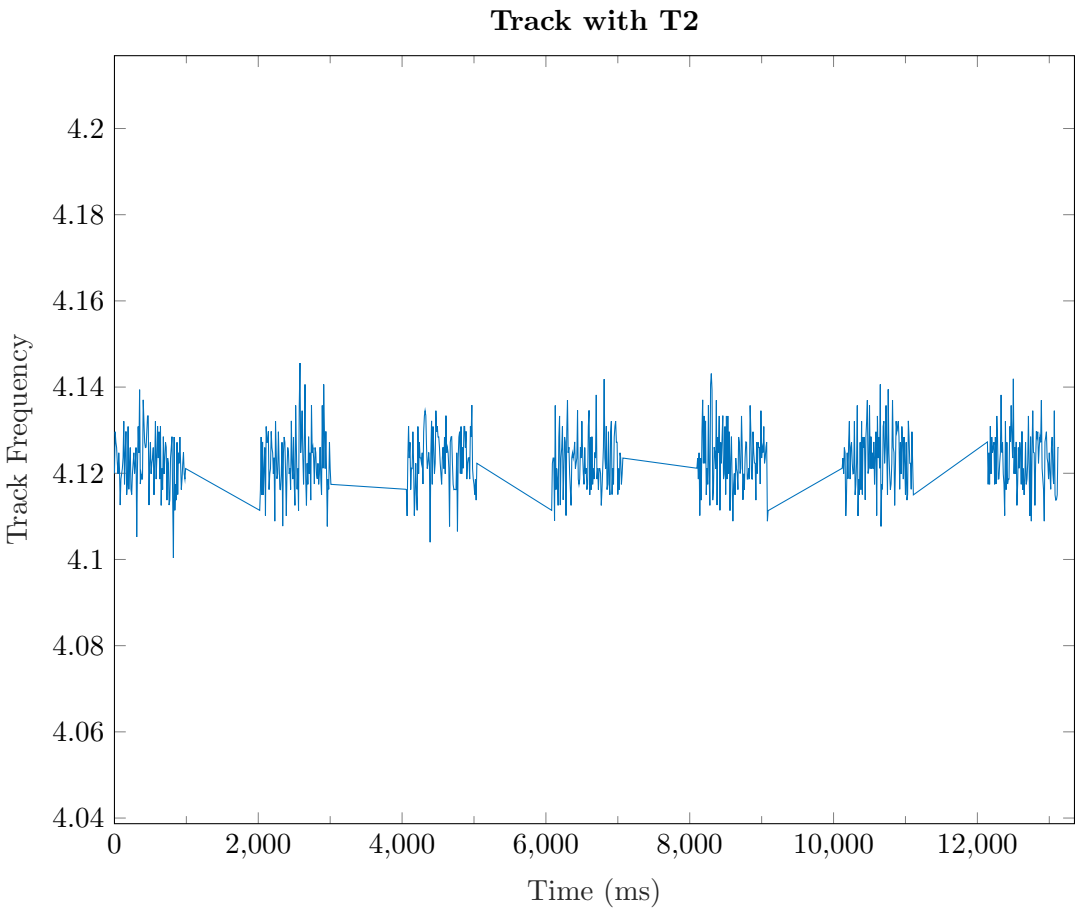

Fig. 5.9: Sample of tracking data

CHAPTER 6

CONCLUSION

The Sweeping Impedance Probe built for the SPORT mission was designed to be a more robust evolution of previous implementations of the impedance probe instrument. The probe was designed with the priority of digital signal processing in place of analog processing that has been used on previous probes. This shift removes some of the offsets inherent in analog components that had to be designed around [12]. Digital processing makes for fewer analog components which comes with less signal noise and less power usage but does require a much more involved digital system than previous probes.

The thesis statement for this research project was : Can a miniature low-power sweeping impedance probe be developed using a high speed ADC and digital signal processing techniques that meets the SPORT mission science objectives? During this research a SIP was designed that moved away from previous analog designs to a primarily digital system. Digital methods were devised that accomplished the same measurement goals as analog methods without the need for over sampling and phase shifting that was required for unbiased analog measurements. The remaining analog components in the design are as minimal as was thought possible while still gathering accurate and sufficiently measurable signals.

From the design and testing presented in this thesis report it is clear that the impedance probe instrument was successfully redesigned and met all defined requirements.

6.1 Potential Changes

During the development of the SPORT SIP there were some decisions that should be reconsidered if the probe was to be built again. First among these is the reconstruction filter used to smooth the output signal. The design has an elliptic low-pass filter which has a rapidly changing phase delay, especially at frequencies close to the cut-off frequency. Elliptic filters have higher phase delays than other filters, such as Butterworth or Chebyshev.

This high phase delay was only worsened by working to minimize ripples in the passband. Working around these phase shifts required extra stages in the digital design to accurately compensate for multiple phase wraps that came with very high phase delay. It would be advantageous for anyone looking to recreate this probe in the future to reconsider the design of the reconstruction filter and if such high phase delays can be reasonably avoided. In order to not need any of the compensation for phase wrapping the reconstruction filter would need to have a phase delay of no more than 90 degrees. By staying under 90 degrees the total response would not cross over the 180 degree wrapping point when at capacitive or inductive impedances.

The present design allowed for more passband ripple than was present, but there likely would still have been need for the phase wrapping compensation as any elliptic filter would still have large delays. In the case of the SPORT SIP, the hardware for the probe was designed first so it was decided to retain the existing filter instead of looking into other options. If this had not been the case the filter would have likely been revisited.

REFERENCES

[1] J. E. Jackson and J. A. Kane, "Measurement of ionospheric electron densities using an rf probe technique," *Journal of Geophysical Research*, vol. 64, no. 8, pp. 1074–1075, 1959. [Online]. Available: https://agupubs.onlinelibrary.wiley.com/doi/abs/10.1029/JZ064i008p01074

[2] O. Haycock and K. Baker, "New ionosphere measurement technique: Plasma frequency probe," *Electronics (U.S.)*, vol. 35, no. 48, Nov 1962.

[3] M. D. JENSEN and K. D. BAKER, "Measuring ionospheric electron density using the plasma frequency probe," *Journal of Spacecraft and Rockets*, vol. 29, no. 1, pp. 91–95, Jan 1992. [Online]. Available: https://doi.org/10.2514/3.26318

[4] K. Balmain, "The impedance of a short dipole antenna in a magnetoplasma," *IEEE Transactions on Antennas and Propagation*, vol. 12, no. 5, pp. 605–617, Sep. 1964.

[5] D. T. Nakatani and H. H. Kuehl, "Input impedance of a short dipole antenna in a warm anisotropic plasma, 1, kinetic theory," *Radio Science*, vol. 11, no. 5, pp. 433–444, May 1976.

[6] P. Nikitin and C. Swenson, "Impedance of a short dipole antenna in a cold plasma," *IEEE Transactions on Antennas and Propagation*, vol. 49, no. 10, pp. 1377–1381, Oct 2001.

[7] J. Ward, C. Swenson, and C. Furse, "The impedance of a short dipole antenna in a magnetized plasma via a finite difference time domain model," *IEEE Transactions on Antennas and Propagation*, vol. 53, no. 8, pp. 2711–2718, Aug 2005.

[8] A. Barjatya, C. M. Swenson, D. C. Thompson, and K. H. Wright, "Invited article: Data analysis of the floating potential measurement unit aboard the international space station," *Review of Scientific Instruments*, vol. 80, no. 4, p. 041301, 2009. [Online]. Available: https://doi.org/10.1063/1.3116085

[9] E. Spencer, S. Patra, T. Andriyas, C. Swenson, J. Ward, and A. Barjatya, "Electron density and electron neutral collision frequency in the ionosphere using plasma impedance probe measurements," *Journal of Geophysical Research: Space Physics*, vol. 113, no. A9, 2008. [Online]. Available: https://agupubs.onlinelibrary.wiley.com/doi/abs/10.1029/2007JA013004

[10] E. Spencer and S. Patra, "Ionosphere plasma electron parameters from radio frequency sweeping impedance probe measurements," *Radio Science*, vol. 50, no. 9, pp. 853–865, 2015. [Online]. Available: https://agupubs.onlinelibrary.wiley.com/doi/abs/10.1002/2015RS005697

[11] D. Farr, C. Weston, T. Nielson, C. Frazier, E. Stromberg, J. Miller, A. Swenson, B. Carrick, W. Nelson, V. Vangeison, T. Evans, W. Cox, B. Byers, J. M. Hidalgo,

C. Perkins, C. Fish, and C. M. Swenson, "Auroral spatial structures probe (assp)," in *2014 United States National Committee of URSI National Radio Science Meeting (USNC-URSI NRSM)*, Jan 2014, pp. 1–1.

[12] J. Martin-Hidalgo, "Sequential quadrature measurements for plasma diagnostics," Master's thesis, Utah State University, Logan, UT, 2014.

[13] Analog Devices, "AD9704/AD9705/AD9706/AD9707 Rev. D," https://www.analog.com/media/en/technical-documentation/data-sheets/AD9704_9705_9706_9707.pdf, 2017, Rev. D.

[14] B. P. Lathi, *Linear Systems and Signals*, 2nd ed. New York, NY, USA: Oxford University Press, Inc., 2009.

[15] Linear Technology Corperation, "LTC2258-14/LTC2257-14/LTC2256-14," https://www.analog.com/media/en/technical-documentation/data-sheets/225814fc.pdf, 2009.

[16] *HB0267 Handbook*, Microsemi, 2017, coreDDS v.3.0.

[17] J. Haws, "Command, control and telemetry for Utah State University's scintillation prediction observation research task (SPORT) mission," Master's thesis, Utah State University, Logan, Utah, 2019.

APPENDICES

APPENDIX A

Included CD

```
/
├── LaTex Project Zip
│   └── Figures
├── Libero Project w/ C Code Zip
├── Schematics PDF
└── SIP_Calibrator_Report.pdf
```